BOTSWANA UNIVERSITY OF AGRICULTURE & NATURAL RESOURCES

Department of Agricultural & Biosystems Engineering (ABE)

Effects of Land-use / Land Cover Changes on Flow and Sedimentation from the Metsimotlhabe River Catchment Using Soil and Water Assessment Tool (SWAT) Model

A dissertation submitted to the Department of Agricultural & Biosystems Engineering in partial fulfilment of the requirement for the degree of Master of Science (MSc) in Agricultural Engineering

(Soil and Water Engineering) stream

By

Ontiretse Maiketso

Student ID: 201200059

Main Supervisor: Prof. R. Tsheko

Co-Supervisors: Prof. K. Mmolawa

Dr. G. Gaboutloeloe

APPROVAL

Main Supervisor's Name and Signature

Date

Co-Supervisor's Name and Signature

Date

Co-Supervisor's Name and Signature

Date

Head of Department's Name and Signature

Date

CERTIFICATION

Main Supervisor’s Name and Signature

Date

Co-Supervisor’s Name and Signature

Date

Co-Supervisor’s Name and Signature

Date

Head of Department’s Name and Signature

Date

STATEMENT OF ORIGINALITY

The work contained in this dissertation was compiled by the author at the Botswana University of Agriculture & Natural Resources between January 2020 and August 2021. It is original except where the references are made and it will not be submitted for the award of any other degree or diploma of any other University.

Author's Name and Signature

Date

ACKNOWLEDGEMENTS

First and foremost, I want to express my gratitude to Almighty God for his boundless generosity and unending kindness in all of my activities, which enabled me to begin and complete this study successfully.

I am very thankful for the guidance, support, encouragement and helpful suggestions of my main advisor Prof. R. Tsheko. I would like to extend my appreciation to my co-supervisors Prof. K. Mmolawa and Dr. G. Gaboutloeloe for their comments and suggestions. I would also like to express my gratitude to my tutors, Mr. J. Aliwa and Ms A. Clift-Hill, for their support and guidance in completing this study.

I would like to extend my gratitude to the Barclays Mogae Scholarship for offering sponsorship to the programme of study and the Department of Agricultural & Biosystems Engineering (ABE) in BUAN for allowing this research to take place in such a creative and innovative environment.

Further, I am grateful for the support from the UNESCO Cross-Cutting Project on "The Application of Remote Sensing for Integrated Management of Ecosystems and Water Measures in Africa" which allowed me to validate the results in the field.

I would like to thank all staff in the Ministry of Agricultural Development and Food Security; Department of Water Affairs and Sanitation; Water Utilities Corporation (WUC); and Department of Meteorological Services; (in Botswana), for providing me with the necessary information for the success of this study.

Thanks to my family, for their love, wisdom and support. I would like to give special thanks to Keamogetse for her encouragement, support, patience, and for helping me to keep the focus on my research. My sincere thanks are also due to all my friends who contributed to the success of this study directly or indirectly. And last but not least, my sincere thanks to my colleague Mr. M. Moesi for his assistance in gathering and preparation of the input data for this study.

DEDICATION

To my daughter, Phalana.

ABSTRACT

This study was undertaken to assess the effects of Metsimotlhabe River catchment Land-use / Land Cover dynamics (2006 and 2018) on the inflow and sedimentation into the Bokaa Reservoir using the SWAT model implemented as ArcSWAT. The ArcSWAT simulation was performed for 13years of recording periods starting from 2006 to 2018 with the first 4years used as a warm-up period, 2010 to 2012 as model calibration period, and 2013 to 2015 as model validation period. The calibration was performed against flow quantity on the model run with 2006-Land-use Land Cover (LULC) (Scenario 1) as input and the best parameter values were applied to the ArcSWAT through the manual calibration tool in ArcSWAT. The calibrated parameters were also applied to the ArcSWAT project created with 2018-LULC (Scenario 2). The statistical model performance measures were computed for the separate periods using the SWAT-CUP model. As a result, the ArcSWAT model was well-calibrated against the flow as indicated by the statistical analysis. With Scenario 1 the R^2 obtained for the calibration, validation, and overall periods were; 0.72, 0.89 and 0.82 respectively, whereas in Scenario 2 the R^2 were 0.69, 0.86 and 0.78 for calibration, validation and overall periods respectively.

The change in LULC that occurred between 2006 and 2018 produced larger peaks of flow and total sediment yield from the catchment. The total sediment yield produced for the entire simulation period increased by 117.2% when the most recent LULC was used (Scenario 2, 2018). These changes could be attributed to a 2.27% increase in built-up areas and an 8.0% and 7.89% decrease in forest and shrubland areas respectively due to the 2% increase in the annual population of people in the catchment. A positive correlation with R^2 of 0.965 was achieved between the sediment yield simulated by the flow-calibrated ArcSWAT and sediment yield derived from applying remote sensing spectral analysis.

Keywords: **ArcSWAT, flow, sediment yield, LULC change, Bokaa dam** and **watershed/catchment**

Contents

LIST OF FIGURES

LIST OF TABLES

ACRONYMS AND ABBREVIATIONS

ArcSWAT	GIS interface for SWAT
DEM	digital elevation model
DN	digital numbers
DWAS	Department of Water Affairs and Sanitation
D_WGS	Dutum _ world geodetic system
E_{NS}	Nash–Sutcliffe efficiency
FAO	Food and Agriculture Organization of the United Nations
GIS	geographical information system
HRU	hydrologic response units
in-situ	on site
LULC	Land-use / Land Cover
MTL	metadata file
NSC	North-South Carrier pipeline
OLI	operational land imager
PPU	percent prediction uncertainty
R^2	coefficient of determination/regression coefficient
RS	remote sensing
SUFI-2	sequential uncertainty fitting algorithm
SWAT	soil and water assessment tool
SWAT-CUP	SWAT- calibration and uncertainty programme
TSS	total suspended solids
USGS	United States Geological Survey
UTM	Universal Transverse Mercator coordinate system
WUC	Water Utilities Corporation

1. INTRODUCTION

1.1 BACKGROUND

Land and water are the greatest natural pair of gifts to mankind as the latter gives value to the former. Soil and Water Conservation is vital for controlling nutrients loss from agricultural land, contamination of water bodies, and reducing the rates of sediments deposition in reservoirs, streams, channels, and ditches (Kebede, 2018). Water is a necessity for most productive uses of land (Khan, 2014). The main constraint to agricultural growth in countries with arid and semi-arid climates is the availability of water rather than land (El Ghonemy, 1998).

As rain falls on saturated ground, or when rainfall intensity exceeds the infiltration rate of the soil, runoff occurs, and the water eventually reaches larger waterbodies such as rivers, dams, lakes, and oceans. This movement takes place in a catchment, which is also referred to as a drainage basin, watershed, or river basin. A catchment defines a zone of land that contains a common set of rivers and tributaries draining to a larger waterbody. Surface water movement in a catchment causes erosion by mobilizing the soil and breaking down rock particles. The movable rock and soil particles are then carried away from areas upstream and are deposited downstream by moving water. This process changes the course of a stream or results in the creation of new landforms. The particles deposited in tributaries and then conveyed by streamflow are generally referred to as sediments (Ffolliott et al., 2013). The transportation and deposition of suspended solid particles by streamflow is then called sedimentation.

Sedimentation is influenced by several factors of soil erosion that include land-use or land cover (LULC), soil condition (erodibility, texture, organic matter content), topography, rainfall, watershed area, and the transportation capacity (Wolancho, 2012; Imanparast & Hassanpana, 2010). The transported sediments eventually fill the reservoir at a certain rate depending on the reservoir design and manipulation of factors that influence erosion in a water basin. Sedimentation as an outcome of altered deposit flow regimes is an undesirable influence that cannot be eliminated but can be mitigated and sustained by appropriate anti-erosion works and the selection of appropriate discharge items (Đorđević & Dašić, 2011). The rate of erosion and soil loss in a watershed upstream can be estimated using the information on sediment yield at the river's outlet. Polluted runoff is known as one of the leading causes of damage to waterbodies (Botter et al., 2007) by transferring weathered elements from their banks by flowing streams (Dastrup et al., 2018).

On a global basis, substantial changes in LULC patterns in river catchments have occurred as a result of continued human development (Wang et al., 2007). These changes are expected to have a significant impact on river flows and sediment transport in a given basin (Ma et al., 2009). Changes in LULC and climate have an impact on hydrological response dynamics in distinct watersheds. The LULC changes in a catchment can have an impact on water supply by modifying hydrological processes such as infiltration, groundwater recharge, baseflow, and runoff (Lin et al., 2007). Destructive LULC change can disrupt the hydrological cycle by increasing or lowering runoff production or, in certain situations, even eliminating low flow (Croke et al., 2004). Surface and subsoil flow rates are affected by ground disturbance. Subsoil flow rates are higher in forests than in other types of vegetation, and also, higher subsoil flow is experienced in cultivated soils than in uncultivated soils with hard surfaces. However, regardless of the vegetation cover, after the earth has been disturbed, especially if native organic matter has been removed, subsurface flow rates decrease (Palamuleni et al., 2011).

Sedimentation is a severe issue for Botswana's agricultural dams, as it affects their storage capacity and useful life (Alemaw et al., 2013). Even though every reservoir is designed with a specific storage capacity for sediment deposition, known as dead storage, a large portion of the sediment may be deposited in areas other than the dead storage (above outlet conduits) for many years of the reservoir's life, and this trend cannot be reversed at a low cost. Due to its flat topography, Botswana's dam storage capacity is among the lowest in the region (Botswana-Water-Sector-Policy-Brief, 2012). All perennial rivers in Botswana are shared with neighbouring countries. Botswana has low water resources due to the country's aridity, and it continues to experience drought years. It also faces increased strain for fresh-water supplies due to fast increasing urbanization and climate change, necessitating some actions to address the situation (Department of Water Affairs - Ministry of Minerals & Resources, 2013). One of these measures is the construction of dams to supplement water resources, which may include consideration of dams' active storage capacities. Therefore, it is necessary to protect the reservoir structures in the country and hydrological processes taking place in the catchments have to be frequently studied. Inflow is expected every rainy season but one has to realize that LULC is also changing continuously with time due to the expanding population, which leads to the destruction of vegetation followed by the building of settlements and roads. Hydrological indicators such as discharge, sediment, and nutrient yields may be utilized to investigate the impact of LULC change. Both on-site monitoring and simulation models can be used to obtain these indicators. Because on-site monitoring is frequently impractical due to its labourintensive, time-consuming, and costly nature, hydrological simulation modelling is gaining favour as a solution to these issues (Pokhrel, 2018).

Hydrological modelling has a lot of scope in quantifying runoff and soil loss from the hills and high slope areas that are inaccessible in a watershed (Ndulue et al., 2015). Although there are numerous watershed models to choose from, model selection is based on the application's goals, resources available, and data availability. Despite Botswana having a flat topography, there are some watersheds in the South-Eastern region of the country with steep slopes and degraded woodlands which are the primary causes of soil erosion and sedimentation in riverbeds. Some of the land-use practices taking place in these areas include deforestation, intensive grazing, and arable agriculture. The topography and change in the land-use practices in the region may affect flow volumes in rivers. The integrated outcome of the hydrological models together with Remote Sensing (RS) and Geographic Information System (GIS) can be of assistance to decision-makers in evaluating the best management practices and designing the necessary structures for soil and water conservation to reduce soil erosion, which leads to high levels of sediment deposits in dams (Yousuf & Singh, 2016). The current trend in determining runoff and sediment yield from a watershed is to employ physically-based, spatially distributed models (Abebe & Gebremariam, 2019; Munoth & Goyal 2020).

Water scarcity and quality (content of suspended solids) have long been a source of concern around the world. (Yan et al., 2013; Huang & Lo, 2015; Pokhrel, 2018; Zhang et al., 2019). The Soil and Water Assessment Tool (SWAT) is one of the most well-known models for analysing the impact of land management strategies on water, sediment, and agricultural chemical yields in vastly complicated watersheds (Tang et al., 2011). The use of a hydrological model to quantify and assess hydrological conditions is currently the most extensively utilized method (Xu et al., 2009). The SWAT model is a useful tool for studying the effects of environmental changes on hydrology and water resources (Liu et al., 2017). It is a widely used model to determine watershed components (Priyanka & Patil, 2016). In watersheds where there is data shortage, the SWAT model is capable of simulating runoff and sediment output well (Prabhanjan et al., 2015). Several GIS interfaces have been established for the SWAT which includes the ArcView interface (AvSWAT), Microsoft interface (MwSWAT), and ArcMap interface (ArcSWAT). However, in this study ArcSWAT was selected for use.

1.2 PROBLEM STATEMENT

Many cities and nations throughout the world are dealing with substantial water supply and quality issues, and LULC change is one of the major human activities affecting them (Dwarakish & Ganasri, 2015). As the ground cover changes with time due to land developments performed by the increasing population, water movement also changes and more pollutants are transported by these moving waters. Most rivers in Botswana flow intermittently following rainfall events, resulting in river flow experienced only during the rainy season (normally between September to March). The southern part of the country experiences a shortage of water as the water resources do not match the demand for water due to the low annual rainfall received. River basins in the area have rocky surfaces and hills.

The catchment of Bokaa dam is prone to serious soil erosion problems because of land-use practices and its topography as it lies in a zone faced with serious land degradation problems *(http://www.fao.org/3/y5744e/y5744e08.htm#TopOfPage*) which may increase the amount of sediment deposition. The accumulation of sediments reduces the water storage capacity of a reservoir (Alemu, 2016), and ultimately reduces the capacity for flow regulation which is critical for assuring the reservoir purposes of water supply, navigation, and flood control (Schleiss et al., 2016). The catchment, which includes major villages of Molepolole, Kanye, Moshupa, Goodhope and Thamaga, is adjacent to the City of Gaborone. The dam provides the area with water for domestic use. Currently, it acts as an emergency supply whenever there is a problem with the North-South-Carrier (NSC) pipeline which conveys water from the north-eastern part of the country to supply the City of Gaborone and its surrounding areas, which comprise a population of 231 592 people (*Population & Housing Census 2011 Analytical Report*, 2014).

Rapid urbanization and population increase over the past decades has resulted in many surface disturbances in the area through the construction of homesteads, industries, and roads. During these activities, borrow pits are dug on the earth's surface for the provision of construction materials, and this is coupled with the abstraction of sand from riverbeds. Because of population growth and the depletion of natural resources by emerging economies, many basins throughout the world are being retrograded (Van Rompaey et al., 2002). Large variations in streamflow rates and the amount of material transported in river basins are frequently caused by increased development and land-use activities (Pazúr & Bolliger, 2017). In the Metsimotlhabe River catchment, there has been an observed increase in farming activities which mirrors the population growth in the area. All the above-mentioned activities affect the movement of runoff water in the area, both in quantity and quality. For correct predictions of sediment transport and deposition, reservoir management, and water treatment procedures, monitoring data for sediment transport to, and yield within, reservoirs are essential (Ongley, 1996). Quantification of dam inflow and sedimentation is thus required for long-term sustainability of water resource developments. This will provide useful data for addressing problems associated with a reduction in reservoir storage capacity and problems associated with the treatment of turbid water.

1.3 OBJECTIVES

The objective of this study was to determine the effects of LULC dynamics (2006 to 2018) on inflow and sedimentation of the Bokaa reservoir using the SWAT model implemented as ArcSWAT.

1.3.1 Specific Objectives

The specific objectives of the study were:

a) To produce LULC maps (2006 and 2018) for the catchment;
b) To calibrate and validate inflows (ArcSWAT) using gauge data;
c) To correlate water quality determined (suspended solids) from the flow-calibrated ArcSWAT model to satellite observations (Landsat 8 OLI).

1.4 JUSTIFICATION OF THE STUDY

Water is a critical resource for Botswana's economic development, yet it is limited and expensive to exploit. In terms of potable water, agriculture, fisheries, poultry, piggery, wildlife management, and habitat for vital flora and fauna, the Bokaa dam, which is located within the Metsimotlhabe River catchment, is extremely important to the city of Gaborone. It serves as an emergency supply of water to the Gaborone region when there is maintenance or fault on the NSC pipeline which conveys water from north-eastern Botswana to the southern region. Because the catchment's resources cross administrative and sectoral planning lines, resource use conflicts have arisen in the utilization of land, water, and other natural resources over time. (Statistics-Botswana, 2016). The catchment also has some small charco dams which are mainly used for agricultural purposes. The majority of inhabitants in the catchment region are farmers who rely on small-scale farming for a living.

The Metsimotlhabe River catchment has undergone changes in LULC as a result of the growth of urban areas and settlements. The dam has also been experiencing reduced inflows, which has led to its drying up at times, it was among the Water Utilities Corporation (WUC) dams that became completely dry during the 2012/2013 rainy season (*Population & Housing Census 2011 Analytical Report*, 2014). High turbidity values are identified in water abstracted from the dam into Mmamashia Water Treatment Plant by WUC. An in-depth evaluation is therefore needed on the quantities of sediments reaching the dam through streamflow and the effects of LULC changes in this area. The results will generate knowledge that could assist in catchment management and in designing strategies to minimize sediment deposition in the dam.

Raletshegwana (2014) assessed the effects of LULC changes on streamflow and catchment morphology in the Metsimotlhabe catchment, which drains into the Bokaa dam, and found that the streamflow and runoff coefficients within the catchment have increased over time as a result of changing LULC. The drainage density of the catchment was found to be increasing with time which implies a faster flow of water through the catchment. Also, a study was carried out in Metsimotlhabe catchment by Phetolo (2009) which focused on the impact of sand extraction on river flow and found that sand extraction is the most likely factor responsible for increased flow in Thamaga stream and increased drainage intensity for the entire catchment. This author also noticed a decrease in sediment discharge by the streams in the catchment over the study period. However, there is an acute shortage of stream pollution documentation resulting from sediment transport as the result of LULC on the watershed. It is hoped that this study will partially fill this knowledge gap.

1.5 SIGNIFICANCE OF THE STUDY

For the prediction, planning, and management of water resources, accurate watershed modelling is critical (M. Yu et al., 2011). Also, quantitative assessment of LULC impacts on runoff generation is vital for water resource development (Babar & Ramesh, 2015). Understanding how LULC changes affect basin hydrology will considerably improve the forecasting of LULC dynamics' hydrological effects for long-term water resource management. (Woldesenbet et al., 2016). Water resources project design and implementation require an understanding of the magnitude of these changes in watershed hydrology especially for a country like Botswana with low and erratic rainfall and limited sites that can be dammed due to the flat topography and an ever-increasing population (currently 2.08% growth rate (*https://www.worldometers.info/world-population/botswana-population/*)).

2. REVIEW OF LITERATURE

This chapter gives an overview of models and modelling selection, some of the existing applied watershed models and their classification, a description of the SWAT model, its studies by different researchers, and provides knowledge of techniques used towards attaining the objectives.

2.1 WATERSHED LAND-USE AND LAND COVER: AN OVERVIEW

Land-use refers to the purpose for which the land is used, but it does not refer to the land's surface cover, whereas land cover refers to the land's surface cover but does not refer to the land's usage. Land-use change can lead to adverse effects on ecosystems (Ndulue et al., 2015). On a global and watershed scale, LULC changes have a harmful impact on climate and natural hazards patterns. Therefore, mapping LULC changes at the watershed scale are needed for a variety of uses that includes land and water resources planning and management. The watershed LULC directly affects watershed hydrology by influencing the amount of runoff and soil loss. Several locations throughout the world are experiencing rapid, broad-scale land cover changes (Mas, 1998). The continuous growth of the world population has affected human development, thus more land is required to cater to this growth and to feed it. The growth, in general, affects land-use change leading to the reduction of forested land or land occupied by natural ecosystems (Yalew et al., 2012).

2.2 RAINFALL-RUNOFF HYDROLOGICAL MODELS

A runoff model is a series of equations that aid in estimating the quantity of rainfall that converts to overland flow as a function of several parameters used to describe watershed features (Devia et al., 2015). Understanding, controlling, and monitoring the quality and amount of water resources can be made easier via runoff modelling (Wolfe et al., 2017). Modelling users can use runoff models to see what happens in water systems as a result of changes in pervious surfaces, vegetation, and weather events. Surface runoff modelling can be challenging at times due to the complexity of the calculations and the numerous interconnected variables involved.

Universal components of a model include; inputs, governing equations, boundary conditions or parameters, model processes, and outputs (Singh (1995), cited by Wolfe et al. (2017)). Knapp et al. (1991) highlighted that the rainfall-runoff model must be chosen based on the project's goal, data availability, study size, output required, and desired simplicity. A model that solely predicts overland flow and ignores subsurface flow is also ineffective if a watershed of concern has large infiltration rates. One of the factors that affect model selection is data availability. This is why simpler models are widely used because fine catch characteristics are unknown or very hard to explore (Rinsema, 2014). Each model type has limitations that may make it inappropriate for a particular project. To identify an appropriate model type to be selected, several factors are required: the data requirements review, physical significance, usability and spatial resolution.

2.2.1 History of rainfall-runoff hydrological models

Hydrological modelling has come a long way since its modest start in the 1850s. Before the 1960s, modelling in watersheds was mainly confined to modelling individual hydrological cycle components (Singh & Frevert, 2003). This was mainly because of a lack of available data and limited computing capability. In 1966, the first Watershed model was reported by Crawford and Linsley, called Stanford Watershed Model (SWM) which later became HSPF (Hydrologic Simulation Package-Fortran) and currently existing as BASINS (Better Assessment Science Integrating Point and Nonpoint Sources) (Singh & Frevert, 2003). In later years, several models have been developed in the U.S whereas many other simulation models for hydrology have been developed mainly in Australia, Canada, England and Sweden.

Since computers were introduced in the 1960s and computing capacity exponentially grew over decades, watershed modelling began to become more comprehensive. Advances were made at an increasing pace driven mainly by easy access to nearly unlimited computer capabilities, sophisticated devices, RS and GIS capabilities (Singh, 2018). The resulting computer capacity made it possible to simulate the entire cycle of hydrology and to start numerical hydrology.

2.2.2 Model classification

Researchers categorize and divide models according to different spatial resolutions, type of input/output, simplicity of the model, and others. Wolfe et al. (2017) classify rainfall-runoff models by the spatial processes and model structure. A rainfalls-runoff model structure is determined by the complexity of the control equations for the runoff calculation, while in the model, spatial processes are determined by the interpretation of the catchment: as lumped, semi-distributed, or fully distributed.

Another way of categorizing rainfall-runoff models may be based on the scope of the models' physical principles. It could be classified as a lumped and distributed model based on the model's space and time parameters and as deterministic and stochastic models based on random variableness, spatial distribution and temporal changes. (Devia et al., 2015).

Knapp et al. (1991) described rainfall-runoff models as event models or continuous simulation models. Event models normally predict the runoff of a particular storm event describing a relatively short space of time during the hydrological record, while simulation models operate continuously for both the rainfall and the inter-storm conditions.

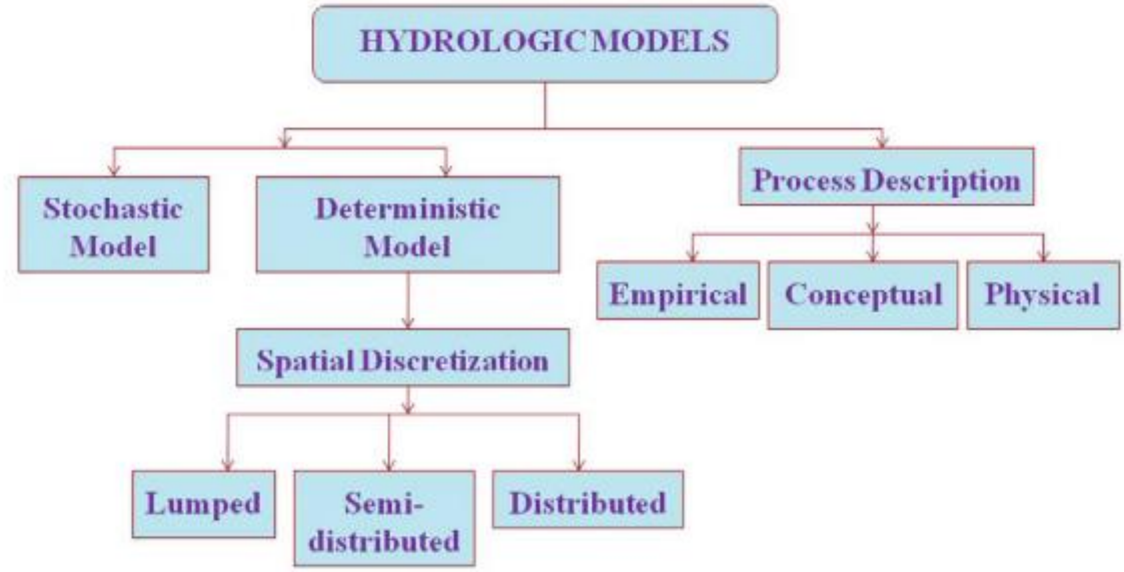

Figure 1: Classification of hydrological models (Dwarakish & Ganasri, 2015)

Table 1: Description of hydrologic models shown above

Model Class	**Brief Description**
Stochastic	The output of these models is at least partially random
Deterministic	Randomness is not considered
Lumped	Generally applied to a single point or a region without dimension for the simulation of various hydrological processes (Niel et al., 2003)
Semi-distributed	Partition the whole catchment into sub-basins or HRUs (Daofeng et al., 2004)
Distributed	The spatial heterogeneity is represented by grids
Empirical	Contain no physical transformation function to relate input to output
Conceptual	They are simplifications of the complex processes of runoff generation in a catchment
Physical	Able to explicitly represent the spatial variability of the important land surface characteristics such as topographic elevation, slope, aspect, e.t.c.

Although there are many classification methods, not all models fit into one category because they have been developed for a range of purposes (Singh, 1995 cited by (Singh, 2018)). The categories are structured according to the model structure including empirical, conceptual and physical structures. The choice of a precipitation-runoff model depends on the purpose of modelling such as the understanding and answer of specific hydrological process questions; the frequency assessment of runoff events; or estimating runoff output for management (Vaze et al., 2011). Dwarakish & Ganasri (2015) reviewed current modelling approaches and summarized hydrological models into broad classes as in *Figure 1*.

2.3 ROLE OF RS AND GIS IN HYDROLOGIC MODELLING

Better elaboration of physical processes in space and time requires the availability of digital products (e.g. distributions of elevation, soil, vegetation) and remotely sensed data (e.g. soil moisture, vegetation), along with new expertise for determining temporal and spatial variability in precipitation (Daofeng et al., 2004). RS may be used for the digital acquisition of spatial information such as soil type and LULC variables that are particularly critical for hydrological modelling (Dang & Kumar, 2017). It offers useful information on LULC dynamics because of its capability of synoptic viewing and repetitive coverage (Shrestha, 2003). RS methods can be utilized to examine satellite imagery and allow a more precise LULC classification. These techniques were effectively used in a range of studies in the prediction of streamflow and sedimentation to support hydrological models (Im et al., 2007; Yan et al., 2013; Worku et al., 2017; Pokhrel, 2018).

The use of GIS has enabled distributed modelling incorporating heterogeneous spatial watershed data including land usage, elevation and soil information (Shrestha, 2003; Chaubey et al., 2005). It is applied to a hydrologic system to assess the influence due to LULC change. Different hydrological modelling techniques enabled GIS users to execute elegant modelling and simulation beyond the data inventory and management stage. The rapid public spread of GIS can increase the transparency of various hydrological models and help to communicate operations and results to a large number of users (Sui & Maggio, 1999).

2.4 HYDROLOGICAL MODELS

There are several useful hydrologic and water quality models available (e.g. MIKE SHE, SWAT, HSPF, ANSWERS, WEPP, etc.) which can simulate temporal-spatial variations in hydrological processes and help to understand the influencing mechanisms behind LULCs (Lin et al., 2015).

Table 2: Examples of hydrological models with their advantages and limitations

Model	Description / Application	Advantages	Limitations / Drawbacks
MIKE SHE (Systeme Hydrologique Europeen)	It simulates the terrestrial water cycle including evapotranspiration (ET), overland flow, unsaturated soil water, and ground-water movements (Z. Zhang et al., 2008).	- It simulates the overland flow processes commonly found in dry regions (Z. Zhang et al., 2008)	- Large data requirements mean that the model is likely to suffer from problems caused by error accumulation
HSPF (Hydrologic Simulation Programme, Fortran)	The model is a catchment scale, a conceptual model whereby catchments are divided into hydrologically homogeneous land segments (Merritt et al., 2003).	- It does not require detailed data on the physical dimensions and characteristics of the flow system (Z. Liu & Tong, 2015).	- Uses hourly historic weather data which is not always available. - The calibration of parameters in HSPF is a strenuous and time-consuming process (Im et al., 2007).
SWAT (Soil & Water Assessment Tool)	A physically-based watershed-scale continuous time-scale model, which operates on a daily time step (Arnold et al., 2012)	- Most of the parameters are automatically generated from GIS data or other information and relatively easy to adjust with proper instruction (Im et al., 2007)	- Proper model implementation requires verification of the model against known output parameters (Yesuf et al., 2015).
WEPP (Watershed Erosion Prediction Project)	A process-based, distributed parameter, single storm and continuous based model used to predict surface flow and sediment yields from the hill slopes and small watersheds (Flanagan & Nearing, 1995)	- Since the model is process-based it can be extrapolated to a broad range of conditions that may not be practical or economical to field tests (Flanagan et al., 1995).	- It requires a large data input which limits its applicability (Rose, 1998).
ANSWERS (Areal Non-point Source Watershed Environment Response Simulation)	A physical model that includes landform information, soil, land-use, and channel description for runoff and sediment transport calculation (Beasley et al., 1980)	- It can be applied over a broad range of conditions because of its flexibility (Beasley et al., 1980)	- The model is mainly designed for agricultural catchments. - Its applicability is limited in many catchments by the large spatial and temporal data requirements (Merritt et al., 2003).

Choosing an application model should be based on the objectives of use (Z. Zhang et al., 2008). Examples and comprehensive information on the model potentials, limitations and applicability, are described in *Table 2*. Data availability for the study area as the main constraint resulted in SWAT being chosen over other models. SWAT was also chosen because of its user-friendliness because most parameters are generated automatically from GIS or other information and can be adjusted with the correct instructions (Im et al., 2007). It was also chosen because of its ability to simulate major hydrologic processes occurring during a rainfall event including precipitation, runoff, streamflow, routing through storage reservoirs (Li et al., 2018).

2.5 SWAT MODEL

The Soil and Water Assessment Tool (SWAT) is a long-term model for continuous simulation of watersheds (Arnold et al., 1993). It was developed by the USDA Agricultural Research Service to predict the impact of land-management practices in large and complex watersheds with different soils, topography, and soil management conditions over longer periods (Neitsch et al., 2011). Bouraoui et al. (2005) describe the SWAT model as soil, water, sediment, and nutrient transformation and fate simulator for agricultural watersheds. Devia et al. (2015) also describe SWAT as a complex physically-based model that examines and predicts water and sediment circulation and agriculture production with chemicals in ungauged basins. The effect of model performance on long-term simulations is said to be more effective. SWAT is an adjustment to the SWRRB model (Simulator for Water Resources in Rural Basin) and includes a new routing structure, watershed flexibility, the transmission of irrigation water, groundwater and lateral flow components (Arnold et al., 1993). SWAT also slots in shallow groundwater flow, reach routing transmission losses, sediment transport and chemical transformations via streams, pools and reservoirs transmissions. Three main components incorporated by SWAT include Sub-basin, Reservoir Routing, and Channel Routing. The sub-basin component comprises eight main divisions: hydrology, climate, sedimentation, soil temperature, crop growth, nutrients, agricultural management, and pesticides. For entering data parameters the SWAT computer interface uses a table layout. As the watershed has no large reservoirs, only the inputs to the sub-basin and the channel routing are discussed.

Yesuf et al. (2015) describe the SWAT model as a continuous river basin/watershed model that is semi-distributed, process-based. In agricultural watersheds with different soil, land-use and management conditions, it has been developed to estimate the impact of land management methods on water, sediment and chemical returns over long-term periods (Arnold et al., 2012). SWAT divides a watershed into several sub-watersheds and then subdivides these into hydrological response units (HRUs), consisting of homogenous land-use, soil management, topography, and soil (Devia et al., 2015). HRU is a unique combination of land-use, soil and slope type in a sub-watershed (Gassman et al., 2007; Neitsch et al., 2011). SWAT produces estimates of hydrology and sediment at the HRU level. Water and sediments are summarized in each HRU and then routed to the outlet of each sub-basin through the stream network. This model was widely applied by researchers in several watersheds to perform different simulations worldwide (Gassman et al., 2007). *Figure 2* describes processes involved in SWAT modelling;

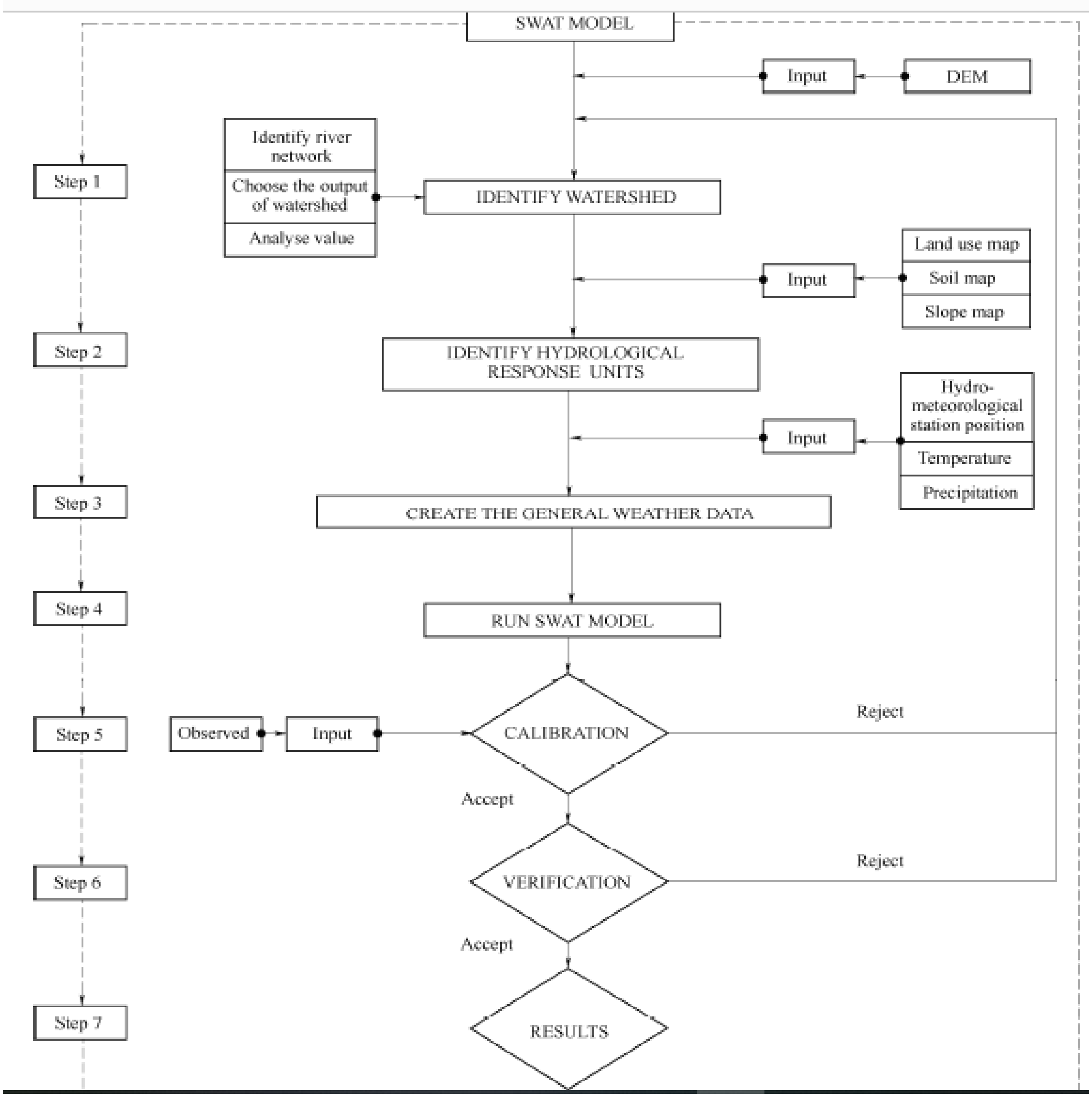

Figure 2: Application of SWAT model (Quyen et al., 2014)

2.5.1 Application of SWAT in hydrological simulation

It is essential to model the possible impacts of LULC change to proceed with effective water resources management (Dwarakish & Ganasri, 2015). Many studies have examined the effect of LULC changes in hydrology and water quality at various spatial and temporal levels. Below are some of the studies that covered the influence of LULC and other factors in the simulation of streamflow and sedimentation or sediment yield;

Van Rompaey et al. (2002) evaluated the contributions of changes in land-use types to changes in streamflow and sediment yield in the Upper Du Watershed (Belgium) using SWAT hydrological modelling and PLSR. Changes to farmland, forest and urban areas from 1978 to 2007 were observed as important land-use changes affecting streamflow, while changes to grasslands did not influence either streamflow or sediment outcome. The tactics employed by this study simply established the contribution of the changes in land-use to streamflow and sediment yields, providing quantitative information to a better knowledge of land and water resource management by decision-makers and stakeholders.

Loi (2010) assessed factors that contribute to reservoir sedimentation, water discharge using the SWAT model in Dong Nai watershed, Vietnam. The study mostly focused on the conversion of forest land-use to agricultural cropping as it is a serious issue experienced by the basin. The impacts of such land-use changes on the surface runoff and sediment yield were monitored. The overall performance of the SWAT model in simulating surface runoff, sediment yield, over time (daily, monthly, and annually) was outstanding. Simulation results indicated that both surface runoff and sediment yield increased when the forest was converted to agricultural land. An increase of about 30% and 54% in surface runoff and sediment yield respectively, occurred when 21% of the forest area was converted to agricultural land. These simulated effects of forest conversion to agricultural land indicate that watersheds in other places having the same pattern of land-use are tormented. The author recommends the implementation of local and national policies to address this problem.

Kimwaga et al. (2012) carried out a study that aimed at characterizing the land-use in the Simiyu catchment of Lake Victoria and using land-uses of 1975 and 2006 and comparing the relative impact of land-use change on sediment loading into the Lake. Characterization of land-uses was performed using RS package ILIWIS 3.0 whereas SWAT was used to quantify the 1975 and 2006 land-use scenarios for sediment loading. The results showed an expansion by an annual rate of change of 2.9% in agricultural land from 19.33% to 73.43% of the catchment.

Moreover, land-use in 1975 generated less sediment load than in 2006. Results show that the model underestimated sediment yield in the catchment.

Bieger et al. (2013) simulated past and future land-use changes in the Xiangxi Catchment (China) with the SWAT model to measure hydrological and sediment transport impacts. In this study, three land-use maps were used based on images by Landsat TM from 1987, 1999 and 2007. The main contributors to the earth loss and sediment outcomes were the cultivated sloping land. Results of simulation have shown a significant increase in sediment yield and surface when areas with slopes < 25% are converted into cultivation.

An integrated approach involving hydrological modelling and partial least squares regression (PLSR) was used by (Yan et al., 2013) to measure the contribution of changes in the different types of land-use to sediment yield and streamflow changes. The study was performed using land-use maps for China's Upper Du watershed from four periods (1978, 1987, 1999, and 2007). Between 1978 and 2007, changes in farming, forest, and urban areas had the greatest impact on streamflow in the examined basin areas, with regression coefficients of 0.232, 0.147, and 1.256, respectively, and a Variable Influence on Projection (VIP) of larger than 1. Farmland (with VIP and regression coefficients of 1.762 and 14.343, respectively) and woodland were shown to have the greatest impact on sediment output (with VIP and regression coefficients of 1.517 and 7.746, respectively). The PLSR technique was found to be advantageous and new because it partially eliminates the co-dependency of the variables and allows for a more unbiased assessment of how changes in specific land-use categories affect streamflow and sediment output. The authors suggested that this approach should be applied to other watersheds where time-sequenced digital land-use maps are available.

Adeogun et al. (2015) did a study that focused on the applicability of SWAT and GIS in the prediction of sediment yield of a watershed upstream of Jebba Reservoir in Nigeria. The model was simulated using 26 years of climatic data (1985 to 2010) from three climate stations set within the catchment. Measured flow data from 1990 to 1995 were used to calibrate and validate the model. A suspended sediment sampler USDH-2A was employed to gather sediment samples from three places in the watershed from May to December 2013 due to the lack of observed sediment data for the area. The samples were examined and utilized to calibrate and validate the model spatially. SWAT was then evaluated statistically using R^2 and E_{NS}. Evaluation of the model revealed that it performed satisfactorily for streamflow and sediment yield predictions in the watershed. The results from the study revealed that a properly calibrated SWAT set in a GIS environment is suitable for modelling the hydrology and predicting the sediment yield in a watershed. It was concluded that SWAT can be used as a decision support tool by water engineers and hydrologists in Nigeria and the surrounding areas to help policymakers achieve sustainable sediment and water management at the watershed level.

The SWAT model was calibrated and validated by Son et al. (2015) in Da River Basin, Northwest Vietnam using observed data from 1971-1981. The results of the assessment have shown that SWAT simulates monthly runoff and sediment output in the study area precisely and is effective for studying the effects of land-use changes on runoff and sediment output as well as for the identification of critical soil erosion areas. Runoff and sediment were increased dramatically by an increase in agricultural land, urban expansion and forest removal, while increased forest cover and practices for soil conservation clarified a drop in runoff as well as the sediment yield.

Huang & Lo (2015) applied the SWAT model to evaluate the effects of land-use change on soil and water losses from Yang Ming Shan National Park Watershed in northern Taiwan. The study simulated the loss of soil and water during two land-use periods (1996 and 2007) with the SWAT Model. The model also simulated the future scenario successfully. The study indicates that forest land decreased by about 6.9%, agricultural land increased by about 9.5%, which influenced sediment yield increase of 0.25 t/ha between 1996 and 2007. The conclusion drawn from the study was that human activities deserve more consideration in the evaluation of the loss of soil and water due to their inevitable consequences. The government was recommended to review land development policies and land-use change detection plans using satellite imaging to prevent illicit development.

Worku et al. (2017) carried a study on modelling runoff–sediment response to LULC changes using integrated GIS and SWAT model in the Beressa watershed. Calibration of the model was performed with data from 1980 to 1999 while the data from 2000 to 2014 were used for validation. LULC maps for 1984, 1999, and 2015 were used in the study, and analysis showed that between 1984 and 2015 agricultural and residential areas increased while grazing, barren and forest areas decreased. However, between 1999 and 2015, forest cover grew. Simulation and calibration of runoff and sediment yield were successfully performed by the model. During the periods of the calibration the values of R^2, E_{NS}, RSR, and PBIAS were 0.72, 0.67, 0.52 and 3.9% respectively. The values were 0.68, 0.64, 0.56, and 7.6%, respectively, at validation periods. The conclusion was that LULC changes had a significant impact on sediment output and runoff.

Nilawar & Waikar, (2018) modified the SWAT model to establish key factors influencing the streamflow and sediment concentration of the Purna basin in India and the potential effects on these factors of future climate and land-use. A SWAT interface domain with GIS was applied for a period of calibration between 1980 and 1994 and validation between 1995 and 2005 to simulate and determine monthly streamflow and sediment concentration. A sequential uncertainty fitting technique (SUFI-2) was further used in the SWAT calibration and uncertainty programme (SWAT-CUP) for calibration and validation. With streamflow simulation, the model performed well with R^2 and E_{NS} values at 0.91 and 0.91 respectively during calibration and 0.83 and 0.82 for the validation period. The sediment data for the basin were also well-presented, with R^2 and E_{NS} being 0.80 and 0.75 for the period of calibration and 0.75 and 0.65 for validation. SWAT can simulate long-term hydrological dynamics in the Purna river basin, according to the research.

The impact of LULC changes was studied by Pokhrel (2018) from the year 2000 to 2010 using the SWAT model. For calibration, monthly discharge and sediment records were used from 1995 to 2002 and the remaining monthly data were used for validation from 2003 to 2010. Four statistical parameters comprising the R^2, E_{NS}, RMSE-observations' standard deviation ratio (RSR), and PBIAS were used for model performance evaluation. The model performed well in simulating discharge during the calibration stage as indicated by R^2 = 0.88, E_{NS} = 0.90, RSR = 0.34, and PBIAS = 0.03. The same performance was also attained with sediment simulation. Results of comparisons with land-use data between 2000 and 2010 demonstrate a reduction of approximately 6.46% of all land-use classes except built-up areas. As a consequence, surface water inputs increased by 27 and 5% to streamflow and sediment output respectively. The expansion of the built-up areas is assumed to increase the contribution of surface water to streamflow, leading to more sediment transportation. This was capable to decrease groundwater contribution to streamflow by 25% because of decreasing infiltration in the catchment.

Sinha & Eldho (2018) studied the impact of changes in historical and forecast LULC for the Netravati river Basin in the Western Ghats of India on monthly streamflow and sediment yield using a SWAT model and six-time land-use maps (1972, 1979, 1991, 2000, 2012, and 2030). The land change modeller with the assumption of normal growth was used for projecting the

2030 LULC. The SWAT model analysis, model calibration and validation have shown that stream and sediment yield in the watershed could be simulated with reasonable efficiency. The spatial extent of the LULC classes of urban, agriculture, and water bodies, increased, whereas that of the forest, grassland, and bare land decreased from 1972 to 2030. The streamflow rose steadily with changes in LULC by 7.88%, while between 1972 and 1991 the average annual sediment yield fell by 0.028% and later rose by 0.029% until 2012. It was found that sediment yield may increase by 0.43% from 2012 to 2030. For the sake of better water resources management plans, the proposed methodology can help other catchments with temporal digital LULCs.

The effect of LULC change on streamflow, sediment, and water quality was evaluated by Boonkaewwan & Chotpantarat (2018) along the Lower Yom River, Thailand. The relative impact of point and non-point sources of pollution from multiple-land-use watersheds were also accessed. Calibration and validation of the SWAT model were performed using data from 2000 to 2013. Land-use change resulted in a 13 to 49% increase in runoff in the catchment and a 37 to 427% increase in sediment yield. Results show that NO3-N loads in the top and middle of the study area doubled, while PO43- ranged between 37 and 377%, reflecting an increase in agricultural and urban areas. The study shows that the changes in land-use are closely related to the amount of runoff, the yield of sediment and the concentrations of NO3-N and PO43-.

Munoth & Goyal (2020) discussed the influences of LULC changes on surface runoff and sediment yield of the Upper Tapi River Sub-basin, India using SWAT. Four land-use maps for 1975, 1990, 2000, and 2016 were used for different scenarios in the study. The four different SWAT models were used with the equivalent climate data between 1979 and 2013 for calibration. Results showed an increase of 18% from 1975 to 2016 for agricultural areas, while forest and rangeland have decreased respectively by 7 and 10%. This change can cause land and environmental damage to the catchment. The model results were evaluated based on the values R^2, E_{NS} and PBIAS, which showed an excellent agreement between observed and simulated discharge. The findings of this study show that changes in LULC have increased surface flow, river discharge and sediment yields. Barren and agricultural land classes for all four scenarios that are responsible for the maximum soil erosion in the catchment have produced the largest sediment yield. The authors concluded that the results of the study could be used in the studied catchment for the conservation of soil and water, and the protection of fluvial health.

dos Santos et al. (2020) reviewed the SWAT model at the Atibaia river basin in (Brazil) to identify land-use-dependent parameters. A sensitivity analysis was performed to determine those parameters with a greater influence on the results of the model simulation and how to consider future conditions for land-use. The most important parameters on stream-flow and sediment output were the initial moisture curve number II (CN), maximum storage canopy per land-use (CANMX) and the cover and management factor (USLE-C). The findings revealed that identification and correct modification in parameters can provide a realistic assessment of the magnitudes of changes in land-use. Such evidence can be used as a tool to improve the environmental quality and management of the basin.

2.5.2 ArcSWAT strengths and limitations

One of the SWAT's key strengths is its ability to model the relative impacts of change in water quantities and quality in management practices, climate and vegetation (Govender & Everson, 2005). Some other significant calibration and validation issues suitable for SWAT applications have been mentioned by Refsgaard et al. (2010), including unrealistic calibration effort due to too many model parameters calibrating. Proper model implementation requires verification of the model against known output parameters (Yesuf et al., 2015) such as using observed actual data experienced in a catchment. One of the challenges attained in SWAT modelling is the need of using a wide range of data and hence include new facilities for the efficient storage, management and handling of extensive data (Devia et al., 2015).

2.5.3 Summary of ArcSWAT use

The SWAT model is a model that is being used worldwide by researchers and hydrologists to perform different simulations in different kinds of catchments. China and India are the countries in which simulation of runoff and sediment is dominant as it seems that most watersheds are gauged in these countries. However, Africa also takes part in making use of the model in the simulation of runoff and sediment yield, most simulation studies in Africa were undertaken in Ethiopia (Bouraoui et al., 2005; Asres & Awulachew, 2010; Setegn et al., 2010; Adeogun et al., 2015; Yesuf et al., 2015; Hailu et al., 2020).

However, there are few publications of SWAT in Botswana concerning the simulation hydrological parameters. The Department of Environmental Sciences at the University of Botswana simulated streamflow (Raletshegwana, 2014). Alemaw et al. (2013) carried out a study using Revised Universal Soil Loss Equation (RUSLE) that aimed at the analysis of prevailing sedimentation processes in dozens of small-dams found in the Lotsane catchment located within the Limpopo River Basin of Botswana and focused on the assessment of annual sedimentation rate. Raletshegwana (2014) assessed the effects of LULC changes on streamflow and catchment Morphology in the Metsimotlhabe catchment.

2.6 ArcSWAT INPUT DATA

2.6.1 Meteorological data

ArcSWAT meteorological data include daytime precipitation, maximum and minimum temperature, solar radiation data, relative humidity and the data on wind speed, which are available from records and/or from simulation data (Neitsch et al., 2011). There is a Weather Generator tool in the model in which generates daily values for weather from average monthly values where only a few meteorological stations in the basin have a full and long record of data (Aduna, 2009). The weather generator uses information found in weather station WGN files.

2.6.2 Topography

DEMs like Shuttles Radar Topography Mission (SRTM) and ASTER describe land-surface topography, which provides vital data on surface-water flow and the interactions of surface water and groundwater (U. Khan et al., 2013). The accuracy of the daily runoff and sediment output values with different DEM resolutions has been reduced. The choice of input DEM data resolution for the SWAT model depends on the output of interest, however, every effort must be made to collect and input DEM data at a finer resolution to minimize uncertainties in the model predictions (Chaubey et al., 2005). For finer DEM resolutions up to 90 m, SWAT is not very sensitive for runoff, but the SWAT outcomes are indeed sensitive for finer DEM resolutions for sediment yield prediction (A. S. Reddy & M. J. Reddy, 2015), hence the DEM of 90m resolution is found suitable for this study.

2.6.3 Soils

The soil's database designates the surface and upper subsurface of a watershed (Hailu et al., 2020). The model ArcSWAT requires various textural and physicochemical properties of soil, such as texture, hydraulic conductivity, bulk density and organic-carbon content for each soil type. (Setegn et al., 2008). SWAT input Soil layer can be prepared by field sampling then the properties may be identified by laboratory analysis, however, there is a national soil layer prepared by FAO which may be obtained from the necessary department (Ministry of Agricultural Development and Food Security).

The soils were mapped under the Soil Mapping and Advisory Services Project of the FAO/UNDP and the soil characteristics were classified regarding the FAO Revised Legends of the Soil Map of the World (Tsheko, 2006). These are the physical properties that include bulk density, particle size distribution, moisture retention, infiltration characteristics and structural stability of the surface soil (Joshua, 1991).

2.6.4 Land-use / Land Cover

LULC classification requires a good awareness of ground conditions and is made more difficult by changing view angles (Kite & Pietroniro, 1996). Information of land-use is an important determinant of hydrologic parameters like runoff, evapotranspiration, soil infiltration and upper soil erosion in the field of study (Hailu et al., 2020).

Classification trees are normally used in classifying different LULC classes. However, the maximum likelihood is the most regularly used parametric classifier in practice, because of its robustness and its easy availability in almost any image-processing software (Lu & Weng, 2007). Training data for directly mapping classification classes are usually performed by interpreting stacks of Landsat images supplemented by high-resolution images from Google Earth (Lu & Weng, 2007; Ying et al., 2017). Ying et al. (2017) outline another way of obtaining reference information for training data for classification as to collect field data over time which is an impractical option for global studies. However, Google Earth has been the most exploited tool in classification by land cover change studies because of the visualizing efficiency of historical change trajectories in the areas of interest (Hansen et al., 2011). In this study, Google Earth is found to be suitable for both training and validation, with Landsat composed images.

2.6.4.1 Image classification programmes

Scientists have made great efforts in developing advanced classification approaches and techniques for improving classification accuracy (Reddy, 1996; Bakker et al., 2001). Classifying remotely sensed data into a thematic map had remained a challenge due to a variety of factors, including the research area's landscape complexity, selected remotely sensed data, and image-processing and classification approach (Lu & Weng, 2007). However, different commercial software programmes have been developed to ease classification (for example, PCI Geomatics, ENVI, ERDAS) and also Freeware is available.

PCI Geomatics: It is a comprehensive and integrated software that includes RS instruments, digital photogrammetry, geospatial analyses, map production, mosaicking, and more. (*https://www.pcigeomatics.com/#*). PCI Geomatics established an easy-to-use and complete software that covers user needs for producing high-quality 2D and 3D geospatial information for GIS, CAD, and mapping applications (Teodoro et al., 2012).

ENVI: It is a programme that visualizes, analyzes, and presents digital imagery of all types. ENVI's complete image-processing package consists of advanced, easy-to-use, spectral tools, geometric correction, radar analysis, terrain analysis, raster and vector GIS capabilities, extensive support for images from a wide variety of sources, and much more (Teodoro et al., 2012). The software embraces essential tools essential for image processing across multiple disciplines, and it flexibly permits the execution of customized analysis strategies (*https://vdocuments.site/documents/getting-started-with-envi.html*).

ERDAS (Earth Resources Data Analysis System) IMAGINE: It offers real value and enhances RS, photogrammetry, Light Detection and Ranging (LiDAR) analyzing, fundamental vector analysis and radar transformation in a single product (*https://www.hexagongeospatial.com/products/power-portfolio/erdas-imagine/erdas-imagine-remote-sensing-software package*).

The three are commercial software programmes that are not freely available. However, PCI Geomatica is available in the Institution where the study is carried out, hence it was utilized for the classification process.

2.6.4.2 Methods of image classification

Unsupervised and supervised image classification are the two approaches used to classify images.

Supervised classification: A variety of supervised classification methods have been applied extensively for land-use change analysis throughout the world (Matlhodi et al., 2019). This technique depends on a combination of background knowledge and personal experience with the study area to a greater extent (Jain & Tomar, 2013). Supervised classification poses a big challenge when there are no suitable land-use maps that could serve as reference maps in the development of training sites and no field verification data. In supervised classification, training samples are selected and the image is classified based on the chosen samples. The training samples are key because they will define which class each pixel inherits in the overall image (*https://gisgeography.com/supervised-unsupervised-classification-arcgis/*).

The maximum likelihood procedure is the most commonly utilized method because of its robustness; nevertheless, it has the underlying assumption of a normal (Gaussian) distribution of the data within each class (Serra et al., 2003).

Unsupervised classification: It produces clusters based on similar spectral characteristics inherent in the image (*https://gisgeography.com/supervised-unsupervised-classification-arcgis/*). Then, each cluster is classified without creating training samples. The main aim is to discover the natural boundaries in attribute space for the number of clusters specified (*https://www.pcigeomatics.com/geomatica-help/concepts/focus_c/oa_classif_intro_unsuper Class.html*). The method is suitable when there is a lack of pre-existing field data for the image area, and the user cannot precisely specify training areas of known cover type (*https://wiki.landscapetoolbox.org/doku.php/remote_sensing_methods:unsupervised_classification*).

2.6.4.3 Accuracy assessment

The accuracy assessment process measures the degree to which features shown on a classification map conforms to what is on the ground (Foody, 2001). However, to offer a reliable classification accuracy report, non-image classification errors should also be inspected, especially when reference data are not obtained from a field survey (Lu & Weng, 2007). Google Earth provides reference images of high resolution for a wide range of time differences and it is time-saving because of no field visiting (Ying et al., 2017).

The most widely used classification accuracy is in the form of an error matrix (Manandhar et al., 2009) as suggested by Story & Congalton (1986). Several accuracy measures such as overall accuracy, user's and producer's accuracy can be derived from this error matrix. The overall accuracy is used to designate the accuracy of the whole classification while the other two methods indicate the accuracy of individual classes. User's accuracy is considered as the probability that a pixel classified on the map represents that class on the ground or reference data, whereas producer's accuracy represents the probability that a pixel on reference data has been correctly classified (Geremew, 2013).

Another accuracy indicator is the kappa coefficient, which is the degree to how the classification results relate to the values assigned by chance (Ismail et al., 2020). The kappa coefficient values range from 0 to 1. If the value equals 0, it denotes no agreement between the classified image and the reference image whereas if it equals 1, then the classified image and the ground truth image are identical. So, the higher the kappa coefficient, the more accurate the classification is (Ismail et al., 2020).

2.6.4.4 LULC change analysis

LULC change is usually performed by applying a change detection procedure. The main aim of change detection is to determine the zones on digital images that change features of interest between two or more dates (Muttitanon & Tripathi, 2005). Several change detection methods have been developed which involve; conventional image differencing, using image ratio, normalized difference vegetation index, principal component analysis, multi-date image classification, post-classification comparison, manual onscreen digitization (Mas 1998; Al-doski et al. 2013).

However, simple LULC change statistics may be used to study the rate at which the LULC types changed in a study where the effect of using images of different times as LULC input in a hydrological model (Geremew, 2013).

2.6.5 Development of hydrological response units (HRUs)

The HRU analysis tool in ArcSWAT is used to load land-use, soil layers, and slope maps to the project. It includes divisions of HRUs by slope classes in addition to land-use and soils.

A threshold is usually selected in defining the HRU (Geremew, 2013; Paul, 2015). The use of threshold levels reduces the number of HRUs in the SWAT model and optimizes the SWAT model as well as the computing demand (Winchell et al. 2013).

2.6.6 Flow data

Streamflow measurement is mostly significant in estimating the hydrology cycle (Negrel et al., 2011). Hydraulic structures are practically installed in rivers with a free water level to predict discharge based on the measured upstream water level (Goodarzi et al., 2012). A measured streamflow datum is essential to calibrate and validate the performance of the SWAT model (Hailu et al., 2020). This data is usually available in Hydrological and Meteorological organizations where the records are kept for research purposes.

2.6.7 Water quality

For water monitoring purposes, sediment can be categorized as deposited or suspended (Ongley, 1996). Deposited sediment is that found on the bed of a river or lake whereas suspended sediment is found in water solution from a waterbody. Suspended sediment is a good proxy for water quality monitoring due to its close association with other water quality parameters (Gao et al., 2018). Methods for water quality monitoring include in-situ, laboratory, and satellite measurements (Robert et al., 2018). For in-situ and laboratory suspended sediment measuring, a variety of instruments are available ranging from simple mechanical samplers to sophisticated optical and acoustical (electronic) sensors (*http://www.coastalwiki.org/wiki/Measuring_instruments_for_sediment_transport*). In-situ sampling permits the investigation of a wide range of parameters at different depths while RS technologies provide frequent synoptic measurements and extend the ability to study remote waterbodies that cannot be visited regularly in a cost-effective way (Bresciani et al., 2019).

Generally, shortage and difficulties to obtain observed water quality data to enable a full spatial calibration and validation at the watershed scale is a major concern worldwide (Neitsch et al., 2011; Mbajiorgu, 2018). However, different RS water quality evaluation techniques have been established and extensively applied (for example, Wong et al., 2005; Jones, 2006; Brezonik et al., 2009; Mao et al., 2012; Bresciani et al., 2019). RS techniques of modelling water quality can be separated into empirical and analytical approaches (Wong et al., 2005; Mao et al., 2012). The analytical approach reviews the bio-optical model which is based on the absorption and scattering of underwater elements and their relationship with spectral wavelengths. The empirical approaches correlate the in-situ measurements with satellite reflectance measurements at certain wavelengths. These approaches include linear regression, single-band method, band-combination method (for example, band-ratio, band difference) (X. Wang & Yang, 2019). However, regression analysis is one of the widely used techniques to determine spectral reflectance and water quality parameter relationship by selecting derived regression models with high R^2 values (Jaelani et al., 2016; Pham et al., 2018). The empirical approach is universally not applicable but can be applied locally and regionally. The constraint of the empirical approach is the requirement of sufficient in-situ data which are not always able to acquire in some remote areas.

RS data have easy access (many moderate images of spatial resolution are free, like Landsat, MODIS, Sentinel and MERIS) but requires some processing to convert measured satellite radiation to water quality information (Bresciani et al., 2019). The reflectance at many different bands is a major suggestion to be used in retrieving total suspended matter (TSM) or turbidity (Ouillon et al., 2008). However, Landsat has a better resolution than the other three sensors described (Kapalanga, 2015) which makes it applicable on small reservoirs such as the Bokaa Dam.

2.6.7.1 Landsat algorithms developed to determine water quality estimates

Turbidity and suspended sediment concentrations are associated with the suspended sediment fluxes in lakes, rivers, and reservoirs, and can assist in monitoring the sediment discharge, and mostly the sediment budget within watersheds (Robert et al., 2018).

Turbidity is generally described as a measurement of water clearness and reflects the degree of cloudiness by sediment (Wong et al., 2005). Prediction of turbidity using different satellite sensors has been widely adopted (Wong et al., 2005; Jones, 2006; Quang et al., 2017; Bresciani et al., 2019).

Suspended sediments have been widely mapped using visible red channels (Wong et al., 2005; Siregar et al., 2019). Also, different regression algorithms for TSS concentrations have been developed based on single-band and two-band ratios reflectance combinations (Jaelani et al., 2016; Pham et al., 2018).

2.7 SWAT CALIBRATION, VALIDATION AND EVALUATION OF THE MODEL PERFORMANCE

The majority of currently used hydrological structures can be classified as conceptual. The algorithms used in these frames contain parameter values often without a direct physical interpretation. The calibration process is necessary to estimate the model parameters until an acceptable level of agreement exists with the system output and model output (Wagener & Wheater, 2006). ArcSWAT is a physically-based, continuously distributed model, therefore data-intensive and its parameters require calibration and validation (Huang & Lo, 2015).

With ArcSWAT 2012 (latest version) programme used for this study, sensitivity analysis, auto-calibration, validation, and uncertainty analysis can be performed using the SWAT-CUP software (Abbaspour et al., 2007). The software permits users to select among five optimization techniques: parameter solution (ParaSol); generalized likelihood uncertainty estimation (GLUE), a Bayesian framework implemented using Markov chain Monte Carlo (MCMC); sequential uncertainty fitting algorithm (SUFI-2) and particle swarm optimization (PSO). However, the SUFI-2 programme is the most widely used method in SWAT-CUP (Chandra et al., 2014; Bonumá et al., 2015; J. Liu et al., 2017; Nkonge, 2017; Luan et al., 2018; de Andrade & Ribeiro, 2020) because it is a comprehensive optimization and gradient search technique capable of simultaneously calibrating multiple parameters and with a global search function (L. Zhang et al., 2019).

The first step in the calibration and validation process is the identification of the most sensitive parameters for a given catchment area (Arnold et al., 2012).

2.7.1 Sensitivity analysis

The objective of the sensitivity analysis is to scan and find the most sensitive parameters that represented key physical processes (Abbaspour et al., 2017). The model includes a sensitivity analysis of input parameters that identifies sensitive parameters concerning their impact on model outputs. Arnold et al., (2012) defined Sensitivity analysis as “the process of determining the rate of change in model output concerning changes in model output (parameters)”. This analysis is performed before calibration, which adjusts the identified sensitive parameters to match as much as possible to the real-world system. Proper attention to the sensitive parameters may lead to a better understanding and better-estimated values and thus to reduced uncertainty (Lenhart et al., 2002).

2.7.1.1 SWAT-CUP

The programme is semi-automated and requires the user to be familiar with the hydrological characteristics of the catchment being modelled. The programme links various procedures, including Sequential Uncertainty Fitting (SUFI-2) to ArcSWAT and enables Sensitivity analysis, calibration; validation, and uncertainty analysis of the ArcSWAT model (Abbaspour, 2015). The degree to which all uncertainties are accounted for is quantified in the SUFI-2 programme, is by a measure called the P-factor, which is the percentage of measured data bracketed by the 95PPU or 95% prediction uncertainty (Memarian et al., 2014). The strength of analysis and calibration of uncertainty is the P-factor. Another way to estimate the strength of uncertainty analysis and calibration is to use the R-factor. The R-factor is calculated by dividing the average thickness of the 95PPU band by the measured data's standard deviation. The goal of the SUFI-2 programme is to use the smallest 95PPU band or uncertainty band to bracket the majority of the measured data. When a simulation matches measured data exactly, the p-factor is 1 and the R-factor is zero. As a result, bigger p-factor numbers and smaller R-factor values suggest a simulation with less uncertainty. The lower and upper 95PPU limits show the parameter ranges that most closely approximate observed flow during calibration. **The second step** is the calibration process (Arnold et al., 2012).

2.7.2 Calibration

Arnold et al., (2012) defined calibration as an effort to better parameterize a model to a given set of local conditions, thereby reducing the prediction uncertainty. In short, it is a technique for reducing the gap between model simulation and observation. (Abbaspour et al., 2017). Through this procedure, it is assumed that the regional model correctly simulates real processes in the physical system (*Figure 3*).

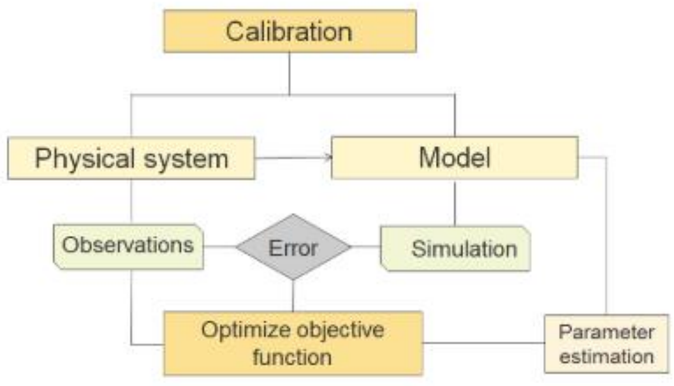

Figure 3: Conceptualization of model calibration (Abbaspour et al., 2017)

The ArcSWAT model can be calibrated manually or automatically. The perfect model calibration contemplates water balance (peak flow, baseflow) and sediment and nutrient transport because calibrating one constituent does not ensure adequate simulation of other constituents during validation (Moriasi et al., 2007). The available data should be considered since the availability of a complete set of hydrologic and water quality data is rare.

Manual calibration involves visual comparison of observed and simulated data (Tolosa, 2015). According to Balascio et al. (1998) cited by Moriasi et al. (2007), manual calibration uses trial and error to adjust the parameters and closeness is evaluated with several criteria and especially recommended for the application of more complicated models in which a good graphical representation is a prerequisite. Manual calibration is tiresome and impractical for large, heterogeneous catchments with many parameters. Consequently, numerous calibration methods have been established to fine-tune adjustable model parameters within user-specified parameter limits to match estimated output to observed hydrologic data (Abbaspour, 2015).

The use of a numerical algorithm to obtain the optimum of a numerical goal function is called automatic calibration (Boyle et al., 2000). This is done by running the model through a variety of combinations and permutations of parameter levels to discover the optimum parameter set that meets the accuracy criterion. All automatic calibration programmes have their advantages, and their usefulness is largely in line with the complexity of both the hydrologic model and the watershed, as well as the computing resources (Barnhart et al., 2018). In this thesis work, automatic calibration is considered for the application.

The final step is validation for the component of interest (Arnold et al., 2012).

2.7.3 Validation

Validation is described as a demonstration that determines how a given site-specific model is capable of making sufficiently accurate simulations; (Arnold et al., 2012; Moriasi et al., 2012). Well-calibrated distributed hydrologic models can be validated on the same catchment with different data series or within the sub-basins where data is available for validation.

2.7.4 Evaluation of the model performance

Many statistics are existing to evaluate SWAT simulation results, for example, Coffey et al. (2004) describe nearly 20 possible statistical tests that can be applied to access SWAT predictions, including coefficient of determination (R^2), Nash–Sutcliffe model efficiency (E_{NS}), root mean square error (RMSE), and others. Nevertheless, the most commonly used statistics have been the R^2 coefficient and the E_{NS} coefficient (Yang et al., 2015). The SWAT-CUP 2019 model can perform these graphical and statistical procedures. According to Moriasi et al. (2007), the R^2 is calculated by regressing the rank (descending) of observed versus simulated constituent values for a given time step and the E_{NS} is calculated as:

$$E_{NS} = 1 - \frac{\sum_{i=1}^{n}(Qobs - Qsim)^2}{\sum_{i=1}^{n}(Qobs - Qobsav)^2}$$ *Equation 1*

Where;

Q_{obs} = observed inflow,

Q_{sim} = simulated flow in m^3/s, and

Q_{obsav} = average observed flow in m^3/s

Hydrologists evaluate model performance to; a) provide a quantitative estimate of the model's ability to reproduce historic and future watershed behaviour; b) to provide a means for evaluating improvements to the modelling approach through adjustments of model parameter values, model structural modifications, the inclusion of additional observational information and representation of important spatial and temporal characteristics of the watershed and c) to compare current modelling efforts with previous study results (Krause et al., 2005). The two statistical methods to be employed for model evaluation are; R^2 and E_{NS} as described by Arnold et al., (2012).

2.7.4.1 Correlation of sediment concentrations simulated by ArcSWAT and derived from satellite images

Due to the lack of sediment concentration records, calibration and validation of sediment concentrations are not possible. However, as an effort to evaluate sediment concentration simulated by the model, these simulated values may be compared to those derived from satellite images using widely applied correlation statistics such as the regression coefficient (R^2) and root mean square error (RMSE) (Jaelani et al., 2016; Hariyanto et al., 2017; Pham et al., 2018; Siregar et al., 2019).

3. MATERIALS AND METHODS

This chapter covers the description of the study area, analysis of different climatic conditions, the hydrological model used, and the methodology adopted to accomplish the aims of the study.

3.1 STUDY AREA

3.1.1 Location of the watershed

The study was carried out on the Metsimotlhabe River catchment which lies between the latitudes 24°15′′0′ S and 25°00′′0′ S and the longitudes 25°05′′0′ E and 26°02′′0′ E. The location of the Metsimotlhsbe River catchment is shown in *Figure 4*. The watershed area that was delineated with ArcSWAT is about 3 610 km^2.

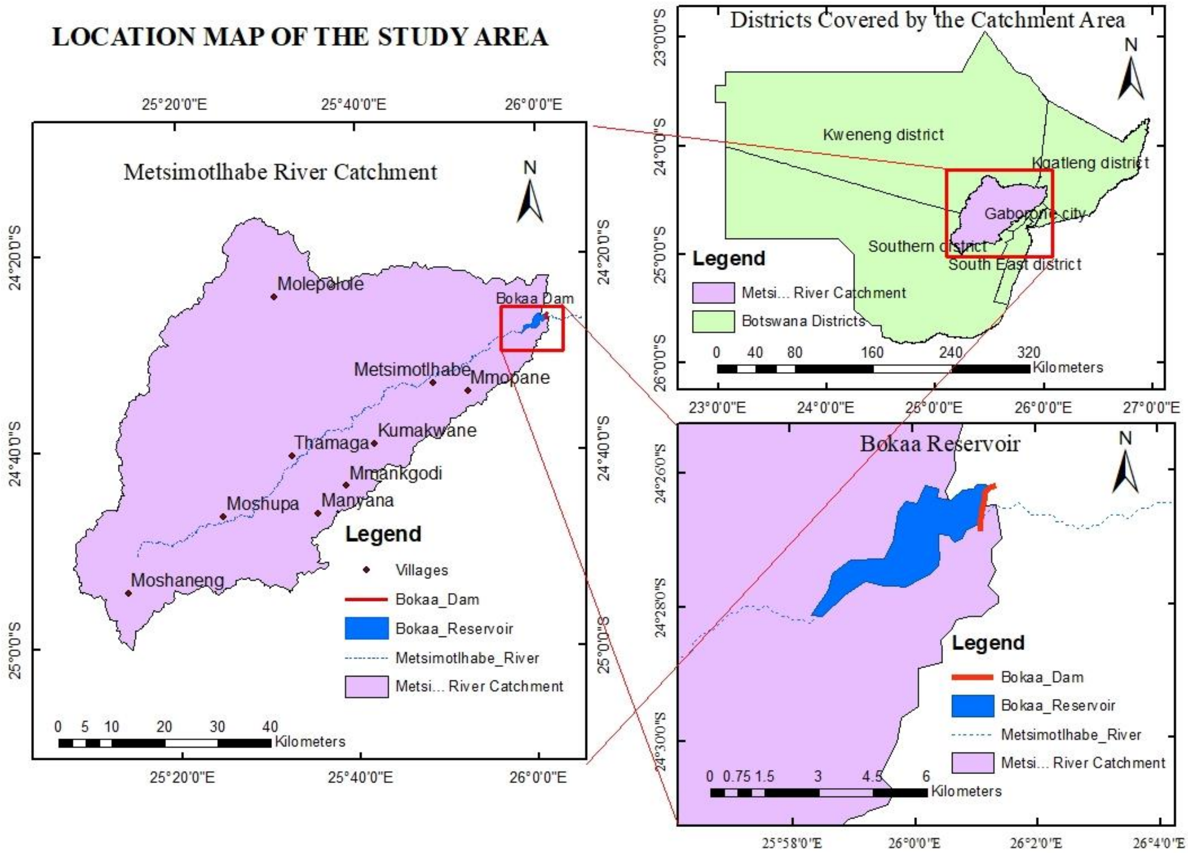

Figure 4: Map of the study area and its location in Botswana

3.1.2 Topography, soil and geology

The topography of the area is more or less undulating uplands with a slope from southwest to northeast, which is crossed by watercourses with hills and rocky hardveld. The elevation of the catchment lies between 946m and 1413m as shown by the elevation map (*Figure 5*).

3.1.3 Water resources

The Metsimotlhabe River catchment is one of the catchments contributing to the flows of the Limpopo River Basin. Metshimotlhabe river is the main tributary that contributes to the inflow with other small tributaries that drains into the Metsimotlhabe river such as the Kolobeng river. There are more than 100 agricultural dams within the catchment that are mainly used to water livestock (Phetolo, 2009).

3.1.4 LULC

The catchment is made up of built-up areas, areas of agriculture, water bodies/dams as well as some tourism-related areas (Raletshegwana 2014). Vegetation is the savanna type with a lot of woody species and is dominated by tree spices which are mostly the acacias (Raletshegwana, 2014) and it is used for grazing livestock including goats, sheep, cattle and donkeys (*https://www.botswana-info.com/country/town/951/bokaa*).

3.2 INPUT DATA COLLECTION AND PROCESSING FOR ArcSWAT

3.2.1 Meteorological data

Meteorological data from the study area that was available for use include daily rainfall (mm) for three stations that fall inside the study area (Moshupa, Sir Seretse Khama Airport [SSKA] and Molepolole) and daily minimum and maximum temperatures (^{o}C) for one station (SSKA). The data (which covers the entire simulation period 2006 to 2018) was obtained from Botswana Meteorological Services and was used as continuous point data input into ArcSWAT. The data was prepared in an Excel sheet and saved in a format accepted by ArcSWAT (.txt). Other weather parameters (wind speed; solar radiation and humidity) were simulated directly by the ArcSWAT model while precipitation and temperature data were fed into it.

3.2.2 Digital elevation model (DEM)

A Shuttle Radar Topographic Mission (SRTM) DEM of resolution 90m by 90m was utilized for providing topographic parameters for the study. A tile of the DEM that covers the study area was prepared with the Raster Projections and Transformation tools in ArcMap. The DEM preparation started by Defining its projection to D_WGS_1984 then it was projected to WGS_1984_UTM_Zone_35S, further, the DEM was resampled to 30m to match other datasets used. The DEM was also used to obtain the watershed slope categories using ArcGIS tools by dividing the slope into 3 classes (0-3%; 3-9%; and >9% (ArcSWAT maximum slope value is 9999%)) as shown in *Figure 5*. The slope classes were then used in the HRU Analysis stage in ArcSWAT to create multiple slopes.

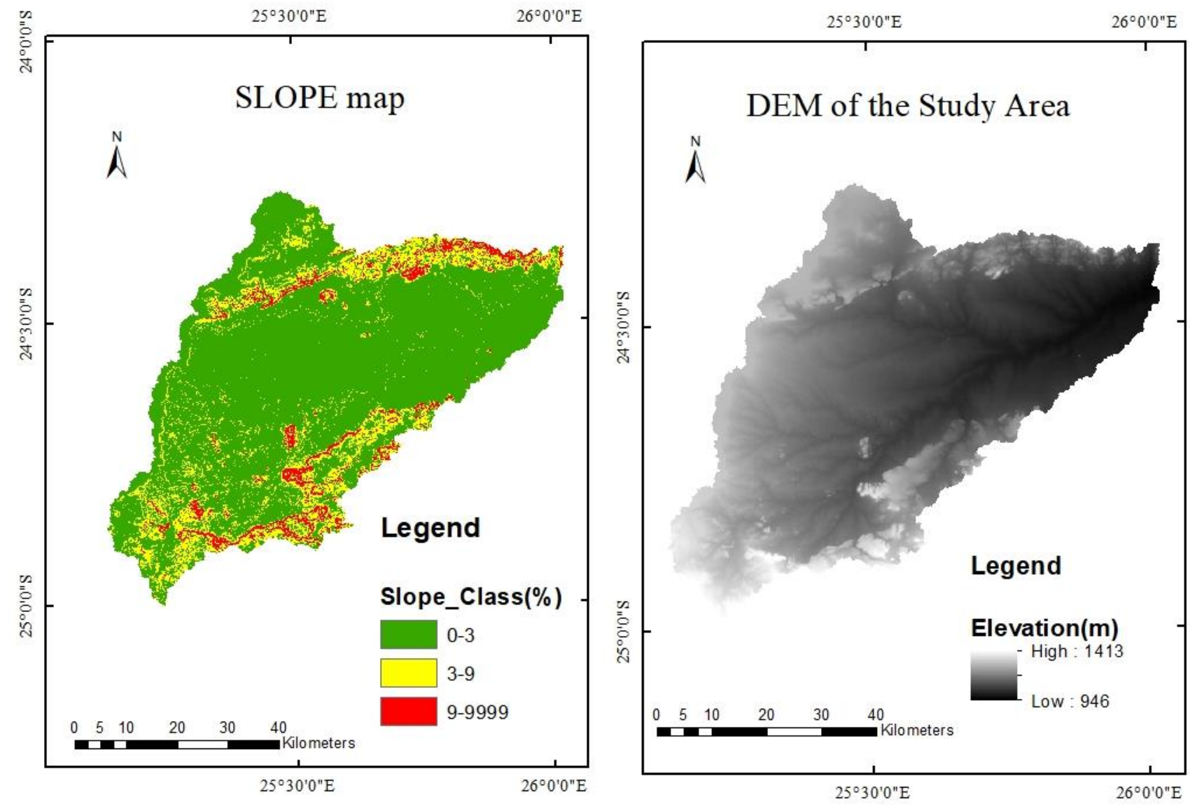

Figure 5: Slope map and DEM of the Metsimotlhabe River catchment

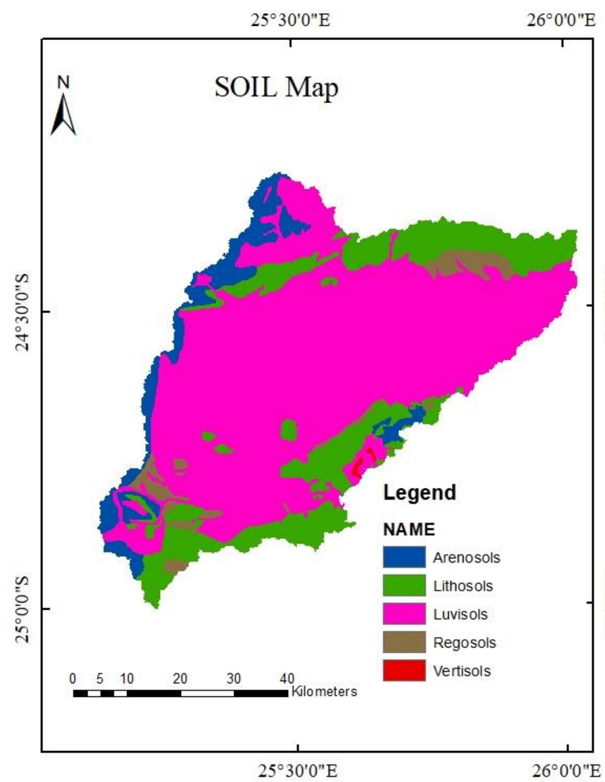

Figure 6: Soil types found in the study area

3.2.3 Soil data

The soil map layer obtained from the Ministry of Agricultural Development and Food Security was reclassified into the Agricultural Research Institute (ARS) land type survey (the different soil classes as defined by ARS) as per the SWAT Input/output Documentation version 2012 (Arnold et al., 2012). The soil classes identified were Lithosol, Arenosol, Luvisol, Regosol and Vertisol as shown in *Figure 6*. ArcMap tools such as dissolve and merge were utilized to produce the five soil types in the study area. A look-up table was then prepared to link the five soil types to the SWAT database.

3.2.4 Land-use / Land Cover data

The LULC data was derived from two Landsat images (for 2006 & 2018), acquired from the United States Geological Survey (USGS) website. These were pre-processed (Collection 1; Level 1) images. For 2006, Landsat 5 image was downloaded and for 2018, Landsat 8 image was downloaded. There was a wide range of Landsat images accessible for download but the issues of availability and accuracy were observed in choosing the images. For instance, Landsat 5 operated from 1984 to 2013 producing images of high accuracy for the entire period. Landsat 6 failed to operate upon its launch in 1993, whereas Landsat 7 started operating from 1999 to date but it encountered some malfunctioning since 2003 and started producing missing data. Landsat 8 was then launched towards the end of Landsat 5 in 2013 and it is producing images of high quality even today (2020) (*https://landsat.gsfc.nasa.gov/a-landsat-timeline/*).

3.2.4.1 LULC mapping

This study employed the use of Geomatica version 2018 in preparing LULC data for input to ArcSWAT. The process of LULC mapping was performed following the method described in the Geomatica Training Guide of 2016. Training data for directly mapping LULC was delineated as class labels by interpreting stacks of Landsat images (for 2006, Landsat 5 image was used and for 2018, Landsat 8 image was used) supplemented by high-resolution images from Google Earth corresponding to the dates Landsat images were captured. Only a single tile of Landsat images covered the entire watershed area (Path_172; Row_77). A global training data set for LULC classification was developed through visual interpretation and on-screen delineation of LULC classes. Landsat false-colour composite images, as well as Google Earth time slider photos, were also used to help interpret the data. Two LULC maps (2006 & 2018) were produced and they were cleaned and smoothed in ArcMap by applying the Generalisation analysis functions to eliminate misclassified features and remove unwanted noise.

3.2.4.1.1 Image classification

The process of classification was initialized as a session in Focus in which Geomatica II software is utilized. Supervised classification following the Geomatica Training Guide (2016) was employed, which involved the following stages; training sites and ground cover, and training site analyses. The training sites were collected based on the researcher's physiographical knowledge of the area with the help of high-resolution images of Google Earth. In addition, image enhancement and composition were applied for better discriminating the land cover classes. The maximum likelihood algorithm was used for classification. *Figure 7* illustrates the supervised image classification steps that were adopted.

Tiles of Landsat images (2006 and 2018) were clipped using a rectangular extent of the study area and the City of Gaborone falls inside the rectangular extent of that clip which made it easier to classify different types of residential areas. This was done to reduce the size of the image that was classified and to improve classification accuracy. Initially, 10 LULC classes were developed which were then merged into five LULC classes in the ArcSWAT database as shown in Table 3.

3.2.4.1.2 Post-classification filtering

Post-classification filtering of image data is used to eliminate noise from a thematic dataset. An FMO filter was applied on the classified images in PCI Geomatica then the image was imported to ArcMap. The images of the study area were clipped from the rectangular extents that were classified in PCI Geomatica. Generalization analysis was performed using ArcMap whereby Majority filter, Boundary clean and Nibble functions were applied.

3.2.4.1.3 Accuracy assessment

The method carried out involved comparing the classified image to a reference image of high resolution from Google Earth. An equally stratified random set of points (30 points each class) was generated from the classified images using ArcMap and classification results were compared with the ground information (Samanta & Pal, 2016; Phinzi, 2018). Google Earth was used to complement found observations because it can be adjusted to match the year on which the image was taken. An error (confusion) matrix accuracy assessment was performed.

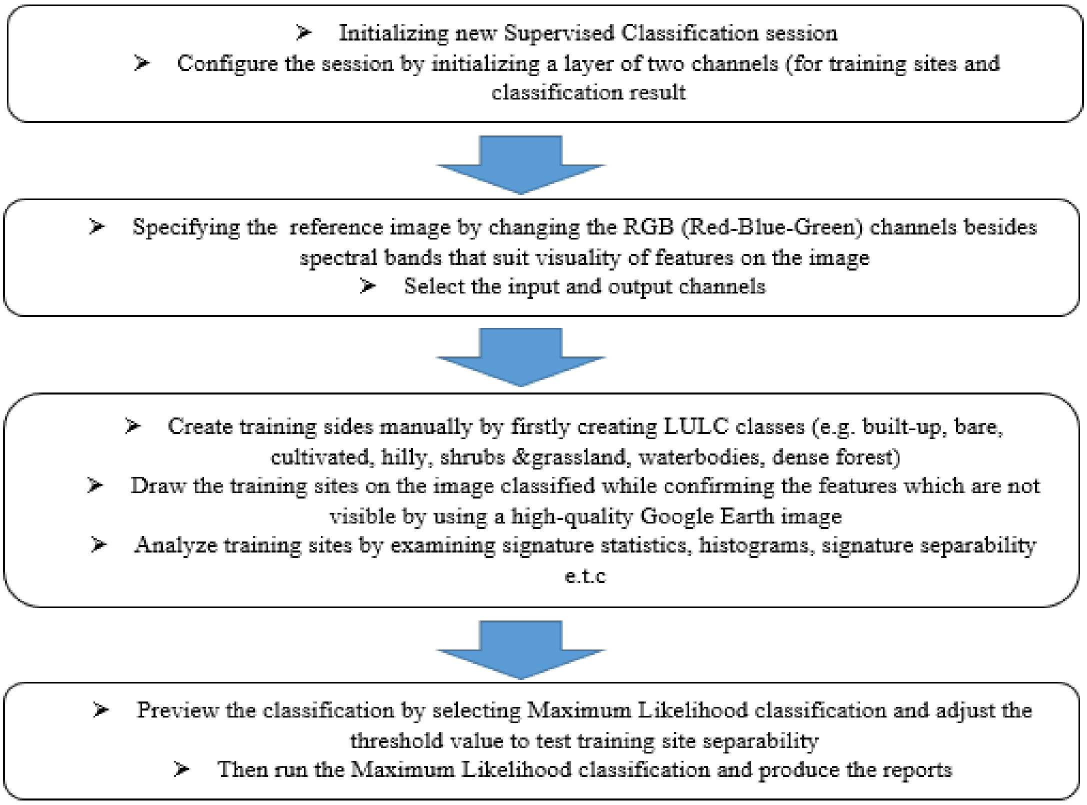

Figure 7: Image classification steps carried out using Geomatica II

Table 3: LULC classes prepared

Initial LULC classes	Areas where training sites were collected	Merged LULC classes	ArcSWAT name
Waterbodies	Dams	Water	WATR
Sewage ponds	Sewage ponds in Gaborone city		
Residential	Residential areas in villages	Built-up	URBN
Industrial	Industrial sites in Gaborone city		
Shrubs	Thorny shrubs mostly growing between cultivated land	Shrubland	SHRB
Tree dominated (hills)	Trees on the sides of the hills, appeared as a shadow in the images	Forest - dominated	FRSD
Tree dominated (rivers)	Tall trees found along the river		
Cultivated land	Cultivated agricultural fields that were bare	Barren or sparsely vegetated	BSVG
Bare	Empty cleared land on the city and borrow pits		
Sparsely vegetated	Bare land covered by few shrubs.		

3.2.4.2 LULC Change analysis

A table that shows the subtraction of areas of LULC classes/types of the latest classified image from LULC classes of the initial classified image was created in Excel (2018 of. 2006).

3.2.5 Hydrological data

3.2.5.1 Streamflow data

Monthly dam level gauge data of the Bokaa dam acquired from the Department of Water Affairs and Sanitation (DWAS) and Water Utilities Corporation (WUC) was used to derive the flow data for the study period. Monthly data for the entire study period was available. However, only dam level data was available and overflow or spillage was not recorded, which means that the inflows were under-estimated whenever the dam was at full capacity and inflow occurred which then spilt away. The data was studied to determine the longest continuous period that the dam did not reach full capacity. A period of six years was identified (2010 to 2015) which was then considered for calibration and validation. This period was split into two halves for calibration (2010 to 2012) and validation (2013 to 2015) of the model. The data was processed in Excel to identify the monthly inflows of the dam with the help of *Equation 2:*

$$Q_{in} = \triangle Q + Q_{out} \qquad \textit{Equation 2}$$

Where;

Q_{in} = monthly inflow,

$\triangle Q$ = monthly change in flow measured by the stage level, and

Q_{out} = monthly flow out from the dam through evaporation, seepage and abstraction (trends were provided by WUC).

3.2.5.2 Sediment data

Water quality data of the water abstracted from the Bokaa dam which is an outlet of the study area was obtained from WUC. The data was limited to turbidity in Nephelometric Turbidity Units (NTU) and total dissolved solids (TDS, in mg/l). The data was insufficient for calibration and validation of the ArcSWAT model because of its inconsistency and gaps as well as the fact that the data needed for calibrating ArcsSWAT are total suspended solids (TSS) which were not available from any organisation that files hydrological data. However, the water quality simulated by the ArcSWAT model was correlated to the water quality of water from the dam retrieved from satellite images.

Turbidity and suspended solids concentration data were derived from surface reflectance from Landsat 8 operational land imager (OLI) images which consist of nine spectral bands. However, the interest was in the first five spectral bands (433 nm, 482 nm, 562 nm, 655 nm and 865 nm) because they were utilized in the regression algorithms which were applied. Surface reflectance (unit-less) is the fraction of incoming solar radiation that is reflected from the earth's surface back to the Landsat sensor (*https://www.usgs.gov/core-science-systems/nli/landsat/landsat-collection-2-level-2-science-products*).

Selection of satellite images required that cloud cover be less than 10% on dates that correspond to the inflows that occurred to the Bokaa dam. Most images that had a cloud cover of less than 10% were for the dry season when there was no flow and only six radiometrically and geometrically calibrated images (Collection 2, Level-2) meeting these selection criteria were downloaded from the USGS website. Landsat Level-2 science products are produced from Collection 2 Level-1 inputs that meet the <76 degrees Solar Zenith Angle constraint and take account of the mandatory auxiliary data inputs to produce a scientifically viable product. Digital number (DN) values were converted to physically meaningful values (surface reflectance) using the Raster Calculator tool in ArcMap. Scaling factors that came with the metadata (MTL) file from the downloaded images were used to rescale the raw DN value to surface reflectance. *Equation 3* shows the algorithm of the scaling factor that was used:

$$R_{rs} = ML(DN) + AL \qquad \text{Equation 3}$$

Where;

R_{rs} = surface reflectance

ML = a multiplicative factor (*0.0000275*) and

AL = an additive factor (*-0.2*) provided in the MTL file.

Surface reflectance at 10 random points in the area covered by water in the Bokaa reservoir was averaged and the best regression algorithms reported in the literature were applied to determine the total suspended solids (TSS) of water in the reservoir.

3.3 DATA ANALYSIS METHODS

3.3.1 Study approach

First of all, input data such as the LULC map (2006), soil and slope maps were prepared with ArcGIS software. The ArcSWAT model version 2012 was then applied to simulate water discharge and sediment yield. The model was calibrated and validated against water discharge using SWAT-CUP software. Finally, LULC in 2006 was substituted by LULC in 2018 to assess the impact of LULC change on water discharge and sediment yield. However, because in-situ data on water quality, including sediment yield, was lacking, the sediment yield calculated by the calibrated model using the two LULC maps was compared to water quality data acquired from Landsat images. The steps involved are summarized in *Figure 8*:

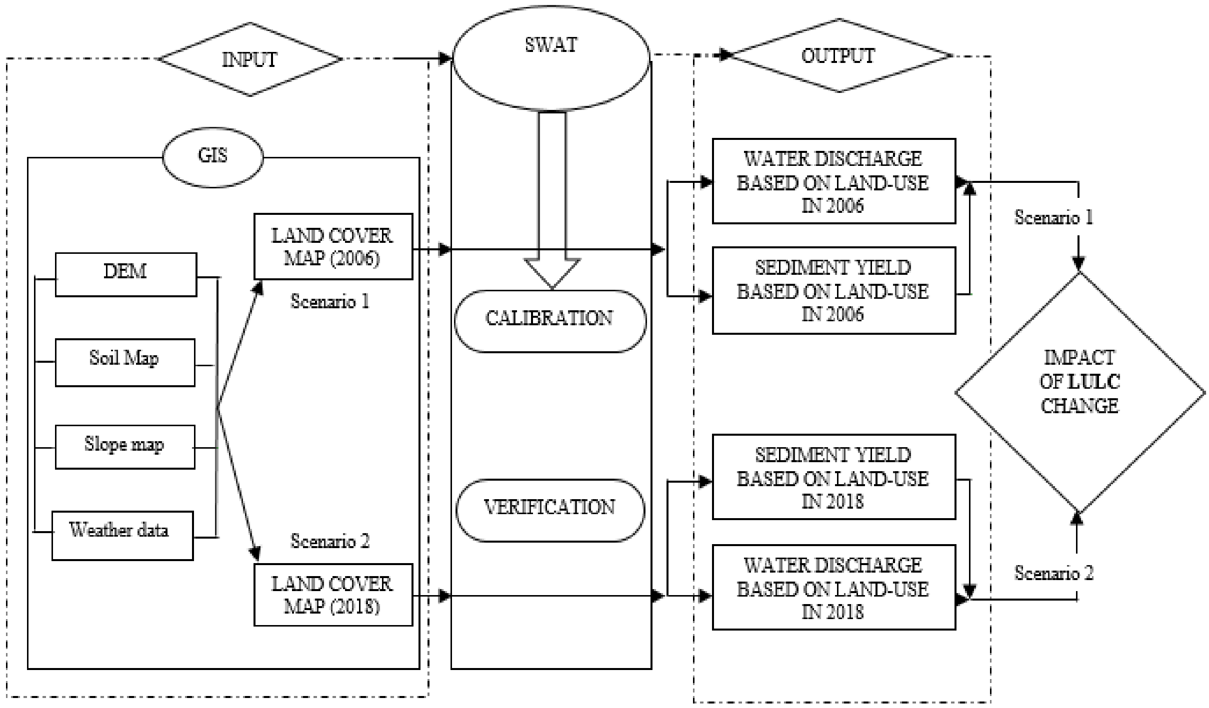

Figure 8: Steps followed when developing the ArcSWAT model for the catchment

3.3.2 Watershed delineation

Inputs entered into the ArcSWAT model (soil, DEM and LULC maps) were organized to have the same spatial characteristics (UTM Zone 35S) and re-sampled to 30m resolution. The first step in creating ArcSWAT model input is to create a new SWAT project in the SWAT Project Setup tool where all the work will be saved. The step that follows is the delineation of the watershed from a DEM. In this process of delineation, a watershed is divided into discrete land and channel segments for the analysis of the behaviour of the watershed. The Metsimotlhabe River catchment was partitioned into several sub-basins (15), for modelling purposes following the Arc SWAT user guide by Winchell et al. (2010). This process involved five major steps: DEM setup, stream definition, outlet and inlet definition, watershed outlets selection and definition, and calculation of sub-basin parameters. For the stream definition, the DEM-based option was chosen to determine flow direction and accumulation. For the outlet selection, a point was created at the Bokaa dam location and it was used to delineate the watershed. *Figure 9* shows the ArcSWAT tools used in watershed delineation:

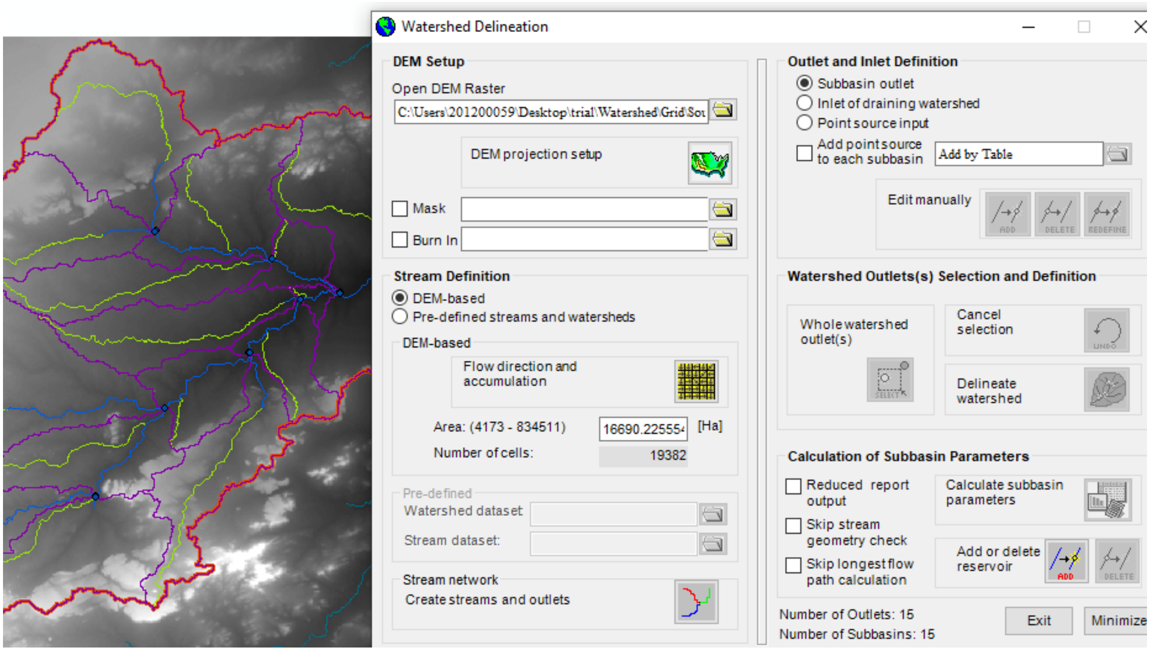

Figure 9: Watershed delineation window

3.3.3 Hydrological response units (HRUs)

HRUs are created using the HRU analysis tool. LULC and soil maps were loaded into the model and LULC types and soil types were linked to the model using the look-up tables that were prepared and Reclassification was performed for both maps to correspond with the parameters in the ArcSWAT database. Then slope percentage classes were derived from the DEM using the Multiple Slope option whereby three classes were formed (0 to 3, 3 to 9 and 9 to 9999). The slope classes were also reclassified and then all the reclassified inputs were overlaid. The step that followed was HRU definition where Multiple HRUs were chosen and a threshold value of 2% was chosen for each of land-use, soil, and slope, as shown in *Figure 10*. HRUs were then created to represent the heterogeneity of catchment characteristics.

3.3.4 Write meteorological data

Metrological data was then loaded into the model in text (tab-delimited) format. The ArcSWAT database was linked to the created layers' data to find all the parameters necessary for estimating the streamflow and sediment yield at each HRU. Data for three rainfall stations and one temperature station that fall inside the catchment were loaded into the model whereas the data for relative humidity, solar radiation and wind speed were simulated by the weather generator tool. Following this, the input tables were written, and the model was set up and the model run was performed in monthly time steps. Details for the model run performance are shown in *Figure 11*. SWAT Output files were then imported to the database and a SWAT check was initiated to examine the hydrology of the watershed.

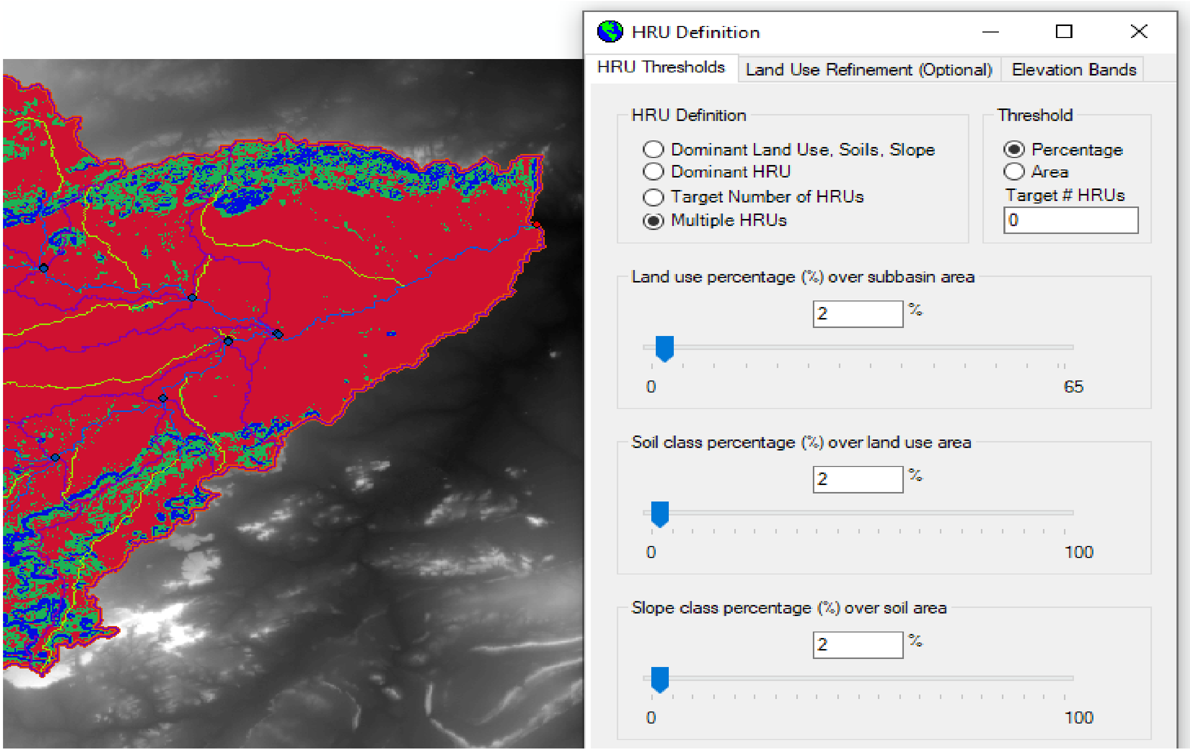

Figure 10: HRU definition window

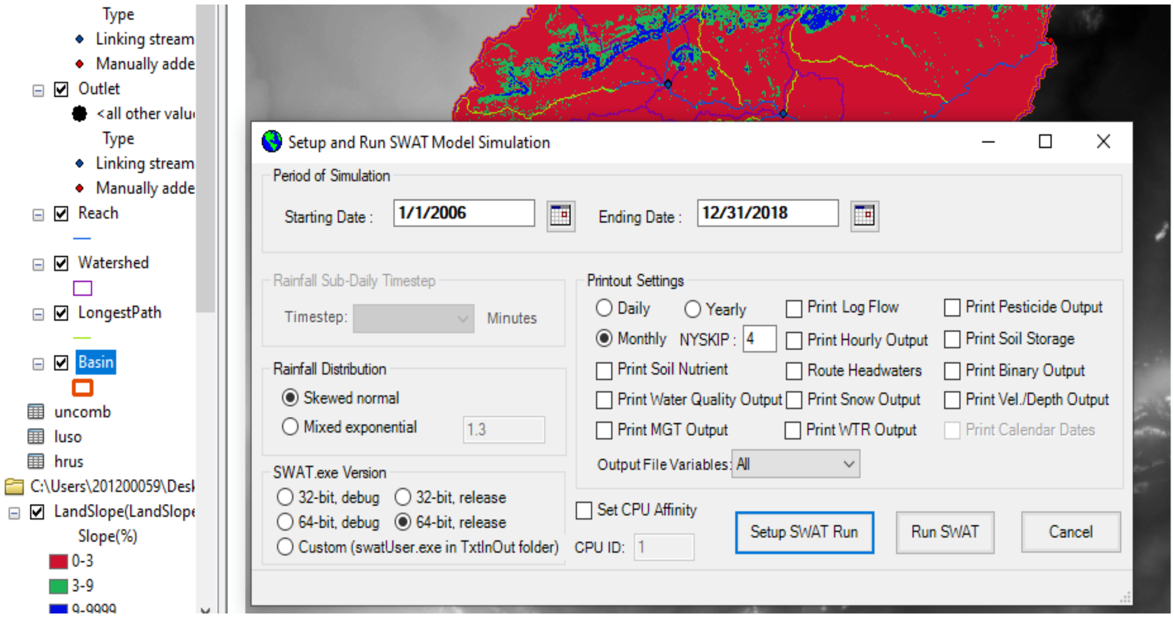

Figure 11: Setup for the model run

3.3.5 Hydrology modelling in ArcSWAT

When rain falls, it can be intercepted and retained in the canopy of vegetation or fall to the ground. (Bokan, 2015). The hydrology model provides estimates of runoff volume and peak runoff rate, which, with the sub-basin area, are utilized in determining the runoff erosive energy variable. Water on the surface of the soil penetrates the profile of the soil or flows as the surface runoff. Runoff moves to stream channels relatively quickly and contributes to short-term stream response. Infiltrated water may be kept in the soil profile and subsequently evapotranspirate or it may slowly find its way to the surface water system via underground pathways (Neitsch et al., 2011).

The first step in developing the hydrological model is defining the basin or watershed boundaries. The demarcated basin is further sub-classified into several HRUs with a unique grouping of LULC, slope, and soil factors. Hydrological parameter simulation at each HRU is performed by employing the following water balance equation given by (Adeogun et al., 2015):

Equation 4

$$SWt = SW + \sum_{i=1}^{t}(Ri - Qi - ETi - Pi - QRi)$$

Where;

SWt = final soil water content (mm),

SW = water content available for plant uptake, which is equal to the initial soil water content minus the permanent wilting point water content (mm),

t = time in days,

Ri = rainfall (mm),

Qi = surface runoff (mm),

ETi = evapotranspiration (mm),

Pi = percolation (mm), and

QRi = return flow (mm).

3.3.6 Modelling sediment loading in SWAT

SWAT predicts sediment yield for each HRU with the modified universal soil loss equation (MUSLE) which evolved from the universal soil loss equation (USLE) developed by Wischmeier and Smith (1965, 1978) as cited by Neitsch et al. (2011). While the USLE uses rainfall as an indicator of erosive energy, MUSLE uses the quantity of runoff to simulate erosion and sediment yield (Kimwaga et al., 2012). The SWAT MUSLE was utilized to determine the amount of sediment at the HRU level as expressed in *Equation 5*:

$$P_s = 11.8\left(Q * P_{peak} * A\right)^{0.56} K_{er} * C_{co} * P_{er} * LS * CF \qquad \textit{Equation 5}$$

Where;

P_s = the sediment yield on a given day (metric tons),

Q = the surface runoff volume (m^3),

P_{peak} = the peak runoff rate (m^3/s),

A = the HRU area (ha),

K_{er} = USLE soil erodibility factor,

C_{co} = USLE cover and management factor,

P_{er} = USLE erosion control practice factor,

LS = USLE slope and gradient factor, and

CF = coarse fragment factor.

3.3.7 Trend analysis of hydrological and meteorological data

3.3.7.1 Data quality checking and validation

Non-homogeneity resulting from either natural or man-made changes to the gauging environment, as well as inconsistency resulting from systematic errors while recording, are both important for effective time series analysis (Wijesekera & Perera, 2012). Users of hydrological must be aware of the risk of observation mistakes, especially when undertaking statistical analysis. Hydrological data quality is managed through reliability checks and correction of missing data and anomalous values.

<u>3.3.7.1.1 Data selection</u>

Acquired data records always have variable quality and record length which necessitates the selection of records to retain a few qualities and considerably long records for the intended study. The data selection process is done a) to obtain a spatially representative data set for the determination of streamflow indices and b) to have the longest and most continuous time series for inter-annual variability analysis concerning land-use patterns. The selection criteria were mainly based on a) record length, b) continuity of records and c) spatial evenness of the distribution of river gauging and recording stations. Some weather data of the study area were abandoned because of short record length data, and some lacked continuity of records.

3.3.7.1.2 Filling missing data

For weather data, the missing data was generated by a weather generator tool. The ArcSWAT weather generator model WXGEN input file contains statistical data needed to generate representative daily climate data for the sub-basins. No data were missing in temperature data for the whole study period (2006 to 2018). However, there were some gaps of missing data in the rainfall records. Where these were outside the rainy season, a zero was recorded while a negative 99 (-99) was inserted for the missing data within the rainy season. This value tells ArcSWAT to generate precipitation for that day.

3.3.7.1.3 Data quality checking and validation.

The accuracy of the results of the study depends on the quality of the input data used in data analysis. Data validation is a process that determines the technical usability of the analytical data. Validation rules should be used to cleanse data before use, to assist with the reduction of "garbage in - garbage out" scenarios (*https://www.safe.com/what-is/data-validation/*). The integrity of data was ensured by checking the range, consistent use of expressions and presence of null values.

In this study, the main data for which it was necessary to check for quality and usability were meteorological and hydrological. Temperature data were visually screened for values that fall outside the expected range and it was found that that the dataset was fine. Rainfall data was also screened and records of erroneous rainfall amounts (such as higher than 500mm per day, not typical in Botswana) were identified and removed. An omission of a decimal point was observed in one of the stations for data records of two rainfall seasons. This was corrected by putting a decimal point where it was necessary.

3.3.8 Statistical measures for the evaluation of results

The SUFI-2 programme in SWAT-CUP was used for sensitivity analysis, calibration and validation of the SWAT model for the Metsimotlhabe River catchment as it performs efficiently in large scale time-consuming models. The inflow data measured in the Bokaa reservoir were the input to SWAT-CUP. Graphical and statistical procedures (R^2 and E_{NS}) were used to evaluate the SWAT model performance several times until values fell within acceptable ranges recommended by Moriasi et al. (2007).

4. RESULTS AND DISCUSSIONS

4.1 LULC

4.1.1 Production of maps

Figure 12 shows the LULC maps for 2006 and 2018 that have been produced from Landsat TM and OLI_TIRS imagery classification respectively. *Table 4* summarizes the individual class areas and change statistics for the two periods from which it can be seen that there was an increase of built-up and barren/sparsely vegetated areas over the 13years of the study period whereas water, shrubland and forest-dominated areas decreased.

By comparing the built-up areas from the two LULC maps in *Figure 12,* the built-up area represented 3.67% of the total watershed area in 2006 which increased to 5.93% by 2018 which is associated with the annual district population growth rate of about 2% (Central Statistical Office (CSO), 2012) (Kweneng and Southern districts contributes the biggest area of the watershed). Population growth encouraged developments such as the expansion of industries, accommodation, and roads/pavements. These developments may also result from rural-urban migration to Gaborone city, which in turn overspills into neighbouring settlements (Keiner & Cavric, 2004) in the Metsimotlhabe River Catchment. This finding is in line with the increase in built-up areas in the Gaborone dam watershed which is adjacent to the study area (Matlhodi et al., 2019). Miller & Hess (2017) concluded that urbanization altered the rainfall-runoff response of a previously rural or low urban density catchment.

Barren/sparsely vegetated areas showed the highest LULC increase of about 8% of the total catchment area over the study period. This LULC type consists of cultivated land, bare land and sparse vegetation. This could be as a result of land cleared for cultivation or as yet unbuilt housing, coupled with increasing bare land due to the establishment of borrow pits for gravel mining and other industrial developments. The trend of expansion of agricultural land irrespective of the economic status and location of the country has been noted by Bessah et al. (2019). Matlhodi et al. (2019) found that expansion in croplands near the study area has been mainly at the expense of the shrubland category which might have also been the case in the Metsimotlhabe River catchment.

On the other hand, the areal coverage of waterbodies decreased slightly, by 0.31km^2 or 0.01% of the total area during the study period. This is in line with the decrease in dam level observed from monthly dam level data acquired from WUC matching the time the Landsat images were

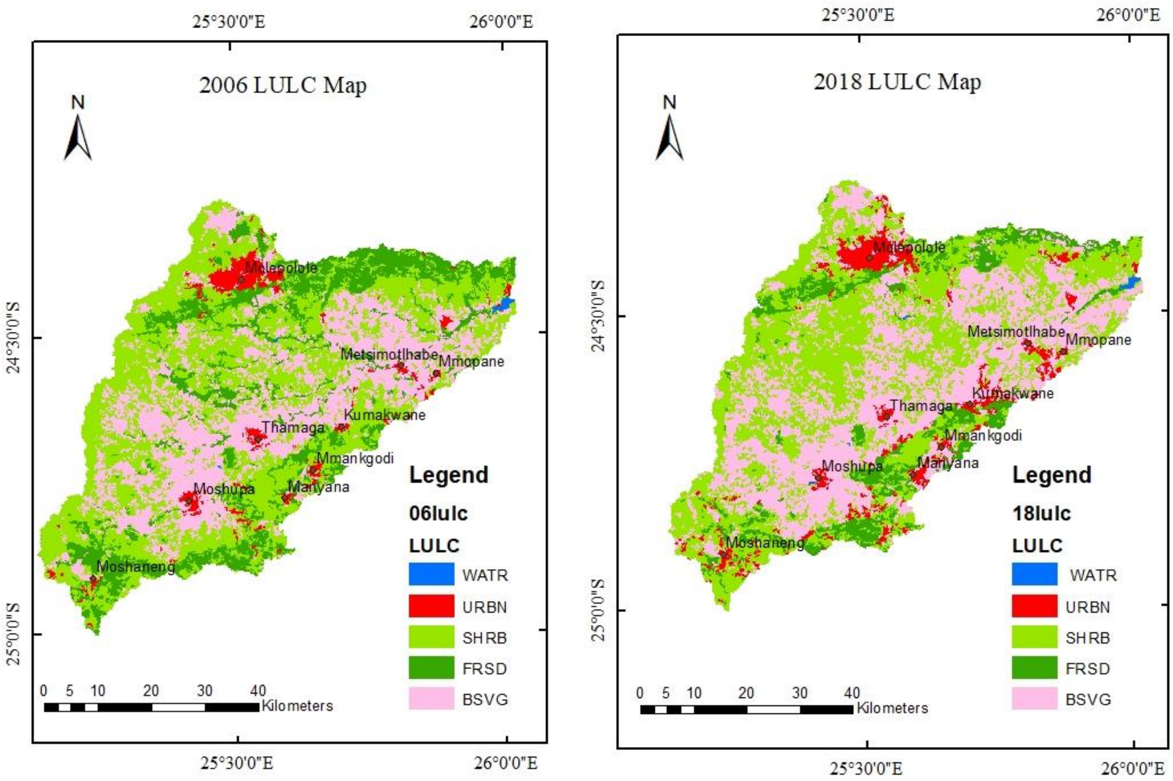

Figure 12: Extent of Land-use / Land Cover types in the study area

Table 4: Area of LULC types, 2006, 2018 and (2018 – 2006)

LULC types	2006		2018		2018 - 2006	
	Km^2	%	Km^2	%	Km^2	%
Waterbodies (WATR)	6.29	0.17	5.98	0.17	-0.31	-0.01
Built-up (URBN)	132.43	3.67	214.22	5.93	81.79	2.27
Shrubland (SHRB)	1671.54	46.30	1590.58	44.06	-80.96	-2.24
Forest-Dominated (FRSD)	647.24	17.93	358.58	9.93	-288.67	-8.00
Barren / Sparse Vegetation (BSVG)	1152.68	31.93	1440.82	39.91	288.14	7.98
TOTAL	**3610.17**	**100.00**	**3610.17**	**100.00**		

captured (July 2006 and July 2018). In July 2006 the Bokaa dam level was at 85% of full capacity whereas in 2018 the dam level was at 73% full capacity. Reduction in dam level is usually associated with a reduction in the water surface coverage of reservoirs. The decline in dam water levels increases the bare land areal coverage (Matlhodi et al., 2019), and as the margins of the Bokaa dam were exposed over the period of this study, the area of bare land

and/or that with sparse vegetation would have increased. Furthermore, these effects may have also occurred with other small dams in the catchment as they dried up.

Natural vegetation (shrubland and forest-dominated) displayed an overall decrease in the catchment during the study period. Reasons for the decline in natural vegetation in the areas around the city are the cutting of live trees for fuel, excessive cutting of firewood by commercial dealers and, the continuous allocation of new farmland because of rising population pressure (Dahlberg, 2000). However, shrubland area losses were previously found to be mainly to croplands in the Gaborone dam watershed (Matlhodi et al., 2019), which is most likely to be the case in this study. Forest-dominated areas experienced the highest loss of coverage by about 8% of the watershed area with shrubland recording about a 2% loss. Forest-dominated coverage loss to shrubland is observed on hills in the catchment as it is visible in the northern part of the study area in the maps shown in *Figure 12*. This may be due to the harvesting of fencing materials (poles and droppers) for croplands as it is observed that people in the catchment are moving away from using shrubs (tree branches) to protect their farming fields and livestock kraals and are instead erecting fences using wire.

These LULC changes may affect water movement in the watershed in different ways. For example, the increase in the bare land area may cause soil erosion and leaching and/or runoff of nutrients and agricultural chemicals in the watershed to groundwater, streams and dams (Foley et al., 2005). The conversion of natural vegetation to built-up areas increases impervious areas, increases runoff, generates pollution and alters the configuration of the watershed (D. Yu et al., 2013; McGrane, 2016).

4.1.2 Accuracy assessment

The accuracy assessment was executed using an error confusion matrix to determine the correctness of the classified images. Using field validation and Google Earth images as a reference, randomly selected points were compared with the corresponding LULC classification. Accuracy indicators such as overall accuracy, user's accuracy, producer's accuracy and the kappa coefficient were determined for both classified LULC maps as indicated in *Table 5* and *Table 6*.

The overall accuracy in this study is greater than 80% for both classified images. However, a high percentage of overall accuracy does not indicate how the accuracy is distributed across the individual categories and cannot be used to judge the accuracy of a classified image (Story & Congalton, 1986).

Table 5: Accuracy assessment results for 2006 LULC map

		REFERENCE DATA						USER'S ACCURACY
		WATR	URBN	SHRB	FRSD	BSVG	**TOTAL**	
CLASSIFICATION DATA	WATR	**30**	0	0	0	0	**30**	**100.0%**
	URBN	0	**25**	2	1	2	**30**	**83.3%**
	SHRB	0	0	**26**	0	4	**30**	**86.7%**
	FRSD	0	0	4	**25**	1	**30**	**83.3%**
	BSVG	0	0	2	0	**28**	**30**	**93.3%**
	TOTAL	**30**	**25**	**34**	**26**	**35**	**150**	
PRODUCER'S ACCURACY		**100.0%**	**100%**	**76.5%**	**96.2%**	**80.0%**		**OVERALL ACC.= 89.3%**
							KAPPA COEF.= 0.87	

Table 6: Accuracy assessment results for 2018 LULC map

		REFERENCE DATA						USER'S ACCURACY
		WATR	URBN	SHRB	FRSD	BSVG	**TOTAL**	
CLASSIFICATION DATA	WATR	**30**	0	0	0	0	**30**	**100.0%**
	URBN	0	**23**	3	1	3	**30**	**76.7%**
	SHRB	0	0	**29**	0	1	**30**	**96.7%**
	FRSD	0	0	0	**30**	0	**30**	**100.0%**
	BSVG	0	1	3	1	**25**	**30**	**83.3%**
	TOTAL	**30**	**24**	**35**	**32**	**29**	**150**	
PRODUCER'S ACCURACY		**100.0%**	**95.8%**	**82.9%**	**93.8%**	**82.2%**		**OVERALL ACC.= 91.3%**
							KAPPA COEF.= 0.89	

4.1.2.1 Producer's and User's accuracy

In this study, the overall result of the producer's accuracy ranges from 80% to 100%. The lowest values for class accuracies were in the barren/sparsely vegetated LULC type and are probably due to misclassification of pixels resulting from the similar spectral values of different land cover classes. The user's accuracy ranges from 76.7% to 100%. Built-up areas (URBN) had the lowest value which was due to some misclassification, because of the similarity in spectral properties of some residential areas and sand which falls under barren or sparsely vegetated (BSVG) LULC class. Also, reeds growing in sewages ponds looked similar to forest-dominated (FRSD) which caused confusion between WATR and FRSD because some training sites for water were taken from sewage ponds.

4.1.2.2 Kappa coefficient and overall accuracy

The kappa coefficient and overall accuracy for the two LULC maps used in this study are greater than 0.8 or 80% which according to Landis & Koch (1977) cited by Mango (2010), represents a strong agreement between the classification map and the ground reference information (thus, kappa values >0.8 [or 80%] represent strong agreement; 0.4 to 0.8 [or 40 to 80%] represent moderate agreement; and values <0.4 [or 40%] represent poor agreement).

Both of the statistical accuracy measures for the 2018 LULC map are greater than the values for the 2006 LULC map (0.89>0.87) which is probably due to the greater spectral resolution of Landsat 8 images than Landsat 5 images (2006-Landsat 5 image had seven spectral bands; 2018-Landsat 8 had 11 spectral bands). This outcome was also observed on the images classified by Matlhodi et al. (2019) while classifying the LULC of an area that is adjacent to the study area.

The overall classification accuracies for 2006 and 2018 are 89.3 and 91.3% respectively. The overall accuracy was higher than the kappa coefficient in both LULC maps. The reason behind this difference is because they incorporate different information, the overall accuracy incorporates the major diagonal only and excludes the omission and commission errors (Mango 2010).

4.2 FLOW ANALYSIS (RUNOFF)

4.2.1 Sensitivity analysis

Sensitivity analysis was performed on flow parameters of ArcSWAT in monthly time steps with observed data obtained from the capacity stage level of the Bokaa reservoir. After a thorough pre-processing of the required input for the ArcSWAT model, flow simulation was performed for 13 years of recording periods starting from 2006 to 2018. The first four years were used as a warm-up period, and the simulation period for both calibration and validation (2010 to 2015) was then used for sensitivity analysis of hydrologic parameters.

Sensitivity analysis was performed before automatic calibration to determine which, amongst a few selected parameters, affect basin hydrology the most and to compare with literature. This study applied the auto-calibration method only. The identification of sensitive parameters was performed using the SUFI-2 programme on SWAT-CUP with the global sensitivity analysis method (Abbaspour, 2015). The results of the sensitivity analysis were used to identify the most sensitive parameters that affected the hydrology of the watershed. Six parameters were selected for the sensitivity analysis with default lower and upper parameter bounds as shown in *Table 7*. These included six parameters that commonly affect the basin hydrology. The upper and lower bounds were chosen with reference to Arnold et al. (2007) and El-Sadek & Irvem (2014). The t-statistic was used to measure the sensitivity of the parameter, where larger absolute values are more sensitive. The p-values indicate the significance of the sensitivity, where p-values close to zero (0) are more significant.

Table 7: Parameters that were involved in Sensitivity Analisis, Calibration and Validation

Parameter		**Upper and Lower Bounds**	**Calibrated Value**	**Rank**
Abbreviation	**Description**			
CN2.mgt	Initial SCS CN2 value	-50 to 50	-9.0125	1
SURLAG.bsn	Surface runoff lag coefficient	0 to 24	0.763175	2
RCHRG_DP.gw	Deep aquifer percolation fraction	0 to 1	0.000125	3
GWQMN.gw	Threshold water depth in the shallow aquifer for flow	0 to 5000	2666.25	4
GW_DELAY.gw	Groundwater delay time	0 to 500	429.85	5
ALPHA_BF.gw	Base flow alpha factor	0 to 1	0.36125	6

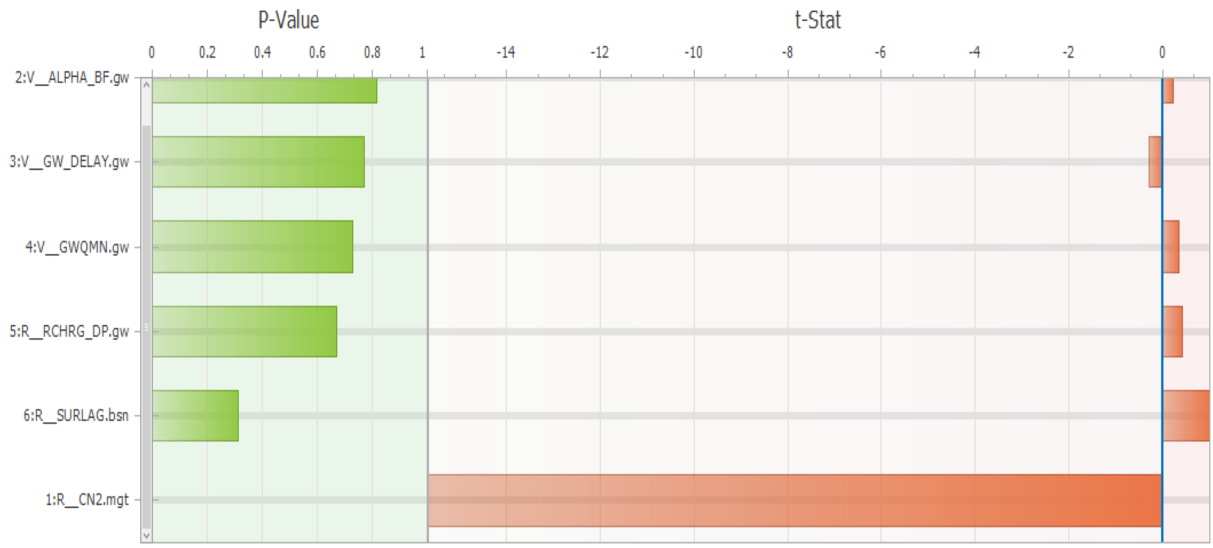

Figure 13: Sensitivity of the parameters involved in calibration and validation of flow

The results of the sensitivity analysis are shown in *Figure 13*, from the SWAT-CUP output display with the sensitivity of the six parameters in descending order. At the top is the base flow alpha-factor (ALPHA_BF) with the highest p-value of about 0.82 and the t-statistic of about 0.2. These p-value and t-statistic values indicate that ALPHA_BF was the least sensitive parameter. The most sensitive parameter was found to be the Curve Number (CN2) which is at the bottom in *Figure 13*, with a p-value of 0 and a t-statistic of about -15.8.

The surface runoff lag coefficient (SURLAG) and CN2 were identified to be the parameters that affect the basin hydrology most because they had p-values less than 0.5 and this indicates that the null hypothesis can be rejected (Grath, 2016). The other four parameters were considered less sensitive because they had p-values greater than 0.5 (*Figure 13*). In most studies, the CN2 is found to be amongst the most sensitive parameters involved in ArcSWAT flow simulation (Geremew, 2013; Tolosa, 2015; Abe, 2017; Anaba et al., 2017; Abusanina, 2018; dos Santos et al., 2020 and others). In *Table 7* the six parameters are listed in descending order of importance in affecting the hydrology of the Metsimotlhabe River catchment.

4.2.2 Flow calibration and validation

ArcSWAT was auto-calibrated using the Latin Hypercube Sampling approach from the SUFI-2 in the SWAT-Calibration and Uncertainty Procedure (SWAT-CUP) package. The calibration was performed on the ArcSWAT model run with 2006-LULC (Scenario 1) as input. First, the parameters were auto-calibrated against the flow for the period of 2010 to 2012 until the model simulation results were acceptable as per the statistical model performance measures as recommended by Moriasi et al., 2007 (*Table 8*). Thus, if the statistics values were below the 'satisfactory' level (*Table 8*), the calibration procedure was repeated. When the statistics values were above 'satisfactory', the model was considered calibrated and was then validated. Once the statistics of both calibration and validation were above ‘satisfactory’, the model was considered ready to simulate the scenarios.

Next, the best parameter values that were calibrated automatically using the SUFI-2 technique were applied to the ArcSWAT project through the manual calibration tool in ArcSWAT and it was re-run for the whole simulation period. The calibrated parameters were also applied to the ArcSWAT project created with 2018-LULC (Scenario 2) and the model was re-run for the whole simulation period. The simulated output was then divided into the validation and calibration periods and the statistical model performance measures were computed for the separate periods using the SWAT-CUP model. The *TxtInOut* directory of the simulations performed with calibrated parameters by ArcSWAT was imported to the SWAT-CUP and the calibrated values for each parameter shown in *Table 7* were set as the minimum and maximum (same value was used as minimum and maximum for each parameter) in the parameter information stage. Statistical measures were also applied on the whole simulation period (calibration + validation periods) for the two calibrated ArcSWAT projects.

The most efficient model (model structure with set parameter) is generally assumed to be representative of the under investigation natural system. Quantitative statistical analyses (R^2 and E_{NS}) were determined to evaluate the model performance as described by Moriasi et al., (2012). *Table 9* shows the results of the statistical model performance measures.

Table 8: The streamflow model performance statistics (monthly time step)

Performance Rating	$\mathbf{E_{NS}}$
Very Good	$0.75 < \mathbf{E_{NS}} \leq 1.00$
Good	$0.65 < \mathbf{E_{NS}} \leq 0.75$
Satisfactory	$0.50 < \mathbf{E_{NS}} \leq 0.65$
Unsatisfactory	$\mathbf{E_{NS}} \leq 0.50$

Table 9: Performance of the flow-calibrated model for the Metsimotlhabe River catchment

	Scenario 1 (2006-LULC)			**Scenario 2 (2018-LULC)**		
	Calibration Period	**Validation Period**	**Overall Period**	**Calibration Period**	**Validation Period**	**Overall Period**
R^2	0.72	0.89	0.82	0.69	0.86	0.78
$\mathbf{E_{NS}}$	0.71	0.80	0.77	0.42	0.82	0.66

The results show that the highest R^2 obtained was 0.89, obtained during the validation period when the ArcSWAT was run with 2006-LULC (*Table 9*). The lowest R^2 was 0.69, which was obtained during the calibration period in Scenario 2 when the model was run with 2018-LULC. According to Moriasi *et al* (2007), R^2 describes the degree of collinearity between simulated and measured data. It ranges from 0 to 1, with high values indicating less error variance and values greater than 0.5 are considered to be acceptable. Thus, all the R^2 values obtained were considered acceptable. For both scenarios, R^2 was found to be lower during the calibration period than the validation period.

The E_{NS} shows how well the plot of observations versus simulated data corresponds to the 1:1 line (Moriasi et al., 2012). The highest E_{NS} value obtained is 0.82 which was obtained during the validation period of Scenario 2 (*Table 8*). The lowest E_{NS} value (0.42) was obtained during the calibration period of Scenario 2 and the model performance was ‘unsatisfactory’ beacause the E_{NS} value was less than 0.50. According to Moriasi *et al* (2007), the performance of the calibrated ArcSWAT model was ‘very good’ during the validation period of the two Scenarios with E_{NS} values greater than 0.75. Also, a “very good” performance was observed during the period when the statistical measures were applied in an overall simulation period of Scenario 1. The calibrated model performance was ‘good’ during the calibration period of Scenario 1 with an E_{NS} value of 0.71 (that is, when the actual calibration process was performed). ‘Good’ performance was also obtained during the overall simulation period of Scenario 2.

4.2.2.1 Output: hydrographs

The hydrographs of simulated and observed monthly discharge for the two scenarios were plotted with the corresponding monthly rainfall received in the catchment. The hydrographs show four major peaks of observed and simulated flows that occurred in Feb-2010, Dec-2012, Mar-2014 and Nov-2015 (*Figure 14* and *Figure* 15) in the two scenarios. The peaks correspond with the high monthly rainfall received in the watershed. The highest observed flow peak was 3.566m^3/s and it was experienced in Nov-2015 and it was in line with the maximum monthly rainfall received in the watershed (136.6mm). However, the maximum simulated flow for the two scenarios occurred during the calibration periods in Apr-2010 which were 2.295 and 3.372m^3/s for Scenario 1 and 2 respectively. Seasonality was visible on the two hydrographs because flow occurred only during the rainy season. No or low flow was observed or simulated during the dry months.

All of the statistical parameters displayed better performance of the calibrated model in Scenario 1 than in Scenario 2 (*Table 9*). The statistics also indicated that the calibrated ArcSWAT model performed better in the validation period than the calibration period. The extended dry season periods that occurred in 2014 and in 2015 (each of about seven months) which were accurately simulated may have played a role in the better performance that was achieved during the validation period (*Figure 14* and *Figure* 15).

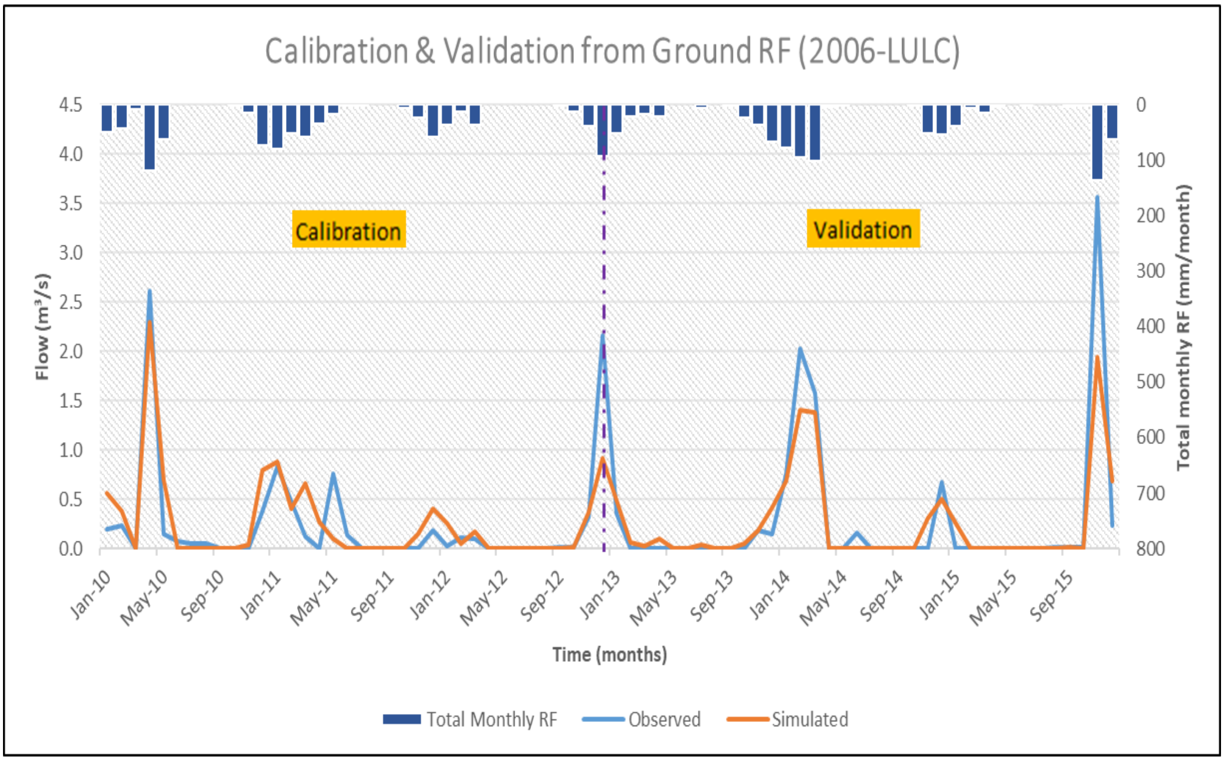

Figure 14: Monthly rainfall and hydrograph for overall simulation using 2006-LULC

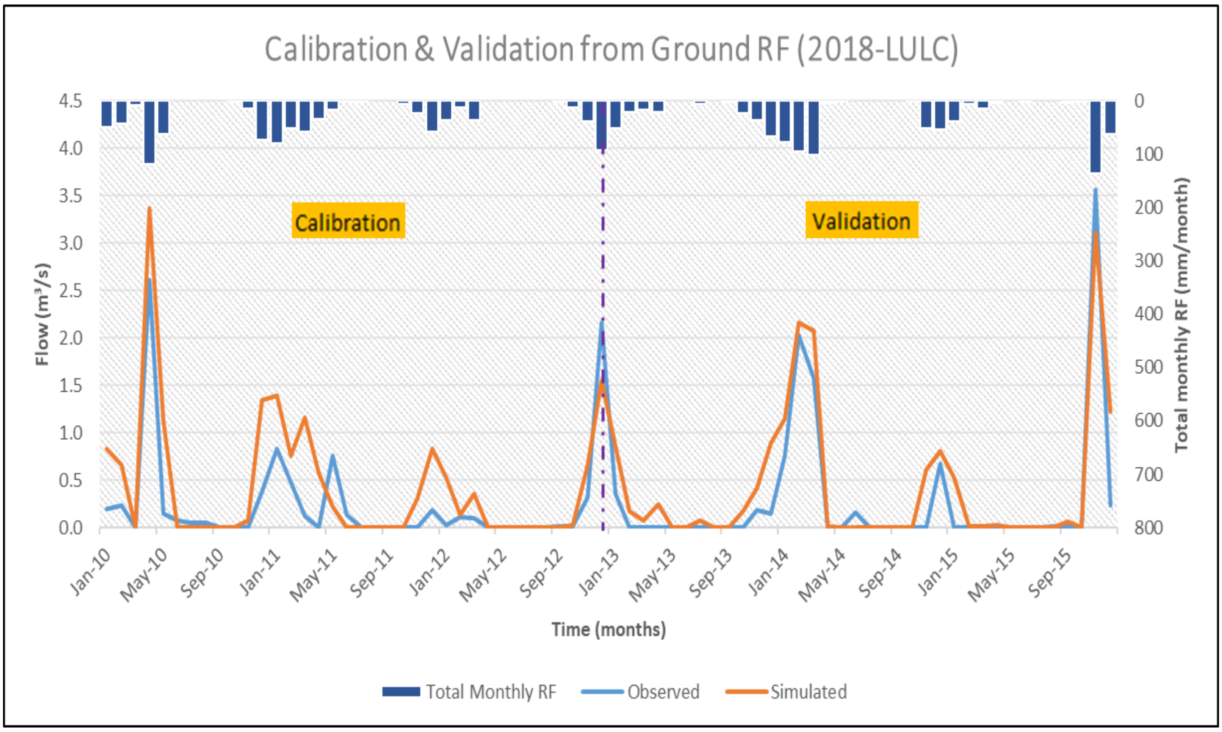

Figure 15: Monthly rainfall and hydrograph for overall simulation using 2018-LULC

Yuan & Forshay (2019) noted that input variables, especially rainfall, may cause uncertainties in model results and in this study, any unidentified errors associated with rainfall data would have been in the calibration period. In mountainous regions, the effect of input uncertainty can be very large (Abbaspour, 2015) and the Metsimotlhabe River catchment is hilly. Nevertheless, the statistical results for the overall period shown in *Table 9* imply that the calibrated ArcSWAT model can simulate the hydrology of the Metsimotlhabe River catchment successfully because of the overall ‘good’ performance established.

4.2.3 Effects of LULC on flow simulation

To evaluate the effects of LULC on flow and sediment yield, LULCs in two different years (2006 and 2018) were used as input variables in the ArcSWAT model. The results showed that peak flows were under-estimated by the calibrated model during Scenario 1 when using 2006-LULC whereas they were over-estimated in Scenario 2 when 2018-LULC was used (*Figure 14* and *Figure* 15). This was influenced by the changes in LULC that occurred during the 12-year interval. Also, low flows were over-estimated except during the long dry periods when no flow occurred.

The increase in LULC (built-up and barren/sparse vegetation) might be reflected by the increase in flow estimates that occurred in Scenario 2. Guzha et al. (2018) observed that cultivated catchments produce higher flow discharge as compared to forest catchments. This is the situation in the Metsimotlhabe River catchment, where barren/sparse vegetation was largely made up of bare cultivated lands, which increased in areal coverage between 2006 and 2018. The results of this study also show that built-up areas increased by 2.27% which might have contributed to the increased peak flow and sediment yield from the catchment. The increase in the built-up area creates impervious layers which reduce infiltration and percolation of water to the shallow aquifers and this effect supports the increased surface runoff found in the Metsimotlhabe River catchment. Anaba et al. (2017) also made the same suspicion in a study that was carried in the Murchison Bay watershed, in Uganda.

The observed decrease of shrubland and forest-dominated vegetation from 2006 to 2018 might cause a reduction in infiltration, resulting in increased dominance of overland flow paths in the study area, leading to higher surface runoff. Deforestation might have also taken place over the study period. According to Guzha et al. (2018), deforestation results in accelerated surface runoff and increase mean annual and peak river discharges, which support the findings of this study.

4.3 SEDIMENTATION ESTIMATION

Sediment transfer takes place predominantly during storm events (Megnounif et al., 2007). Sediment yield simulated by the flow-calibrated ArcSWAT for the entire simulation period (2006 to 2018) with both scenarios was related to the corresponding monthly rainfall as shown in *Figure 16* (the first four years were used as warmup period, hence excluded from the Figure). The results show that sediment yield in Scenario 2 (2018-LULC) almost doubled as compared to Scenario 1 (*Table 10*). The two sediment yield hydrographs show three major sediment yield peaks which correspond to the high monthly rainfall received by the Metsimotlhabe River catchment. The peaks are in April-2010, Nov-2015 and Feb-2017. The highest monthly sediment yield occurred in Nov-2015 for both Scenarios, which was 302.5 and 620.6 tonnes in Scenario 1 and Scenario 2 respectively. However, this did not correspond to the highest monthly rainfall received in the catchment because the highest rainfall was recorded in Feb-2017.

Table 10: Total sediment yield period (2010 to 2018) with the two scenarios

Sediment Yield for the entire simulation period; Scenario 1 (2006-LULC)	**Sediment Yield for the entire simulation period; Scenario 2 (2018-LULC)**
3 295.12 tonnes	**7 157.73** tonnes

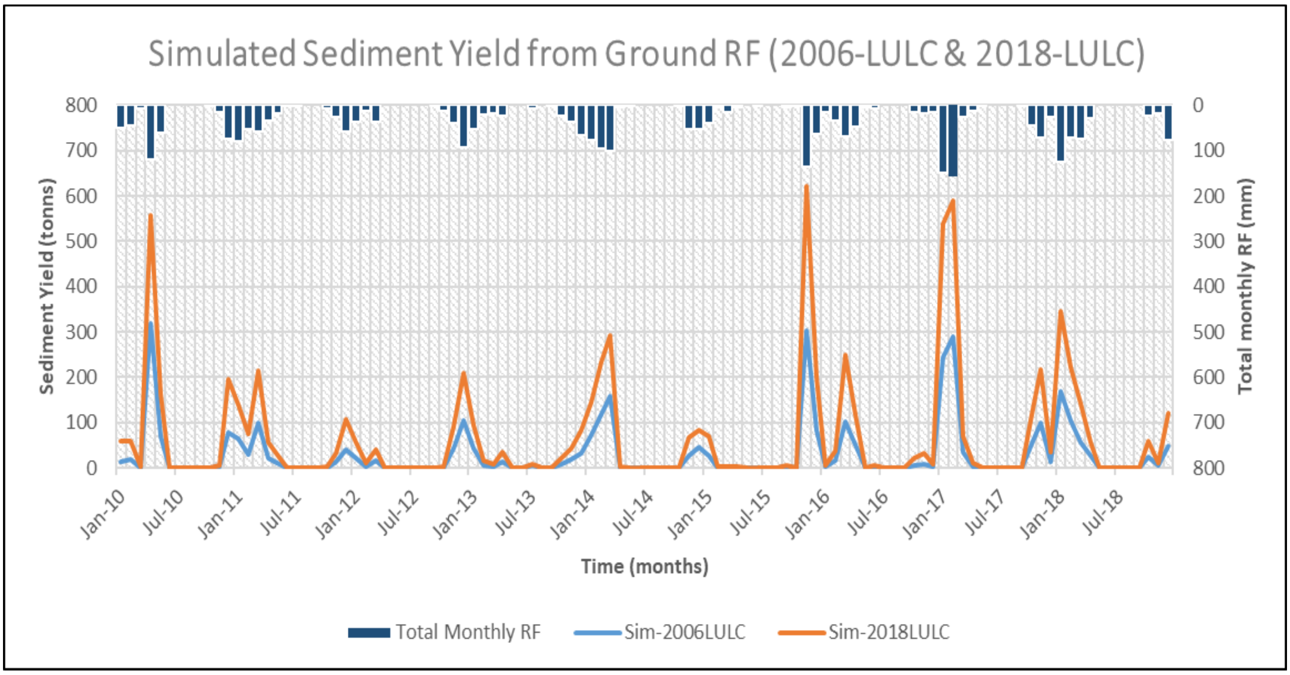

Figure 16: Monthly rainfall and sediment yield simulated with the two scenarios

Megnounif et al. (2007) highlighted that following the dry season, autumn's first rains have important impacts, including splashing soil particles on exposed and desiccated soil. This is in line with what the results of this study show as it can be seen from *Figure 16* that the highest sediment yield occurred from the first rains that followed the dry season period with a monthly rainfall of about 136.58mm (Nov-2015) whereas the highest monthly rainfall that occurred in Feb-2017 (157.21mm) did not produce the highest sediment yield. This rainfall occurred in the middle of the rainy season by when the land had some soil moisture and some seasonal vegetation which offered protection to the soil against mechanical erosion. Duru (2015) supports this finding by highlighting that rainfall influences the rate of relative erosion from drainage catchments across diverse climatic areas as it correlates with vegetation type and density.

4.3.1 Effects of LULC on sediment simulation

It is known that surface runoff is the carrier of all components that affect water quality and as it increases, all these components, including sediment transport will increase, depending on the activities taking place in the catchment (Anaba et al., 2017). In this study, the total sediment yield for the entire simulation period was 3 295.12 tonnes in Scenario 1 and it increased by more than 100% (117.2%) in Scenario 2 to about 7 157.73 tonnes (*Table 10*). This implies that soil erosion was much higher in Scenario 2 when the model was run with the 2018-LULC.

The expansion of the built-up areas is assumed to have increased the contribution of surface water to streamflow, leading to more sediment transportation. Moreover, the increase in sediment yield might be attributed to the decrease in forest and shrubland cover because Chiwera (2015) found a strong negative correlation between a reduction in forest land area and sediment yield. Forest vegetation can efficiently intercept and store runoff and sediment, which reduces the amount of runoff volume and sediment discharge (Xiaoming et al., 2007). Abari et al. (2017) also stress that removing forest canopy cover significantly increases runoff and sediment yield. A review carried out by Negese (2021) revealed that the expansion of cultivated land at the expense of shrubland, forest land, and grassland in Ethiopia has amplified the rate of soil erosion, sediment yield, mean annual streamflow, annual surface runoff, mean wet monthly flow, and water yield in the last four decades, which may also be the case in the Metsimotlhabe River catchment.

4.3.2 Correlation between TSS simulated by the flow-calibrated ArcSWAT and TSS derived from Landsat satellite images

Different algorithms have been developed and widely applied to identify the relationship between surface reflectance as recorded by different satellite sensors and the water quality (turbidity, TSS and TDS) of waterbodies (Pham et al., 2018; Hariyanto et al., 2017; Quang et al., 2017 and others). A total of 15 algorithms were applied to the six Landsat 8 images (2013 to 2018) that met the selection criteria (Section 3.2.5.2) in estimating the TSS (mg/l) in the water that was in the Bokaa reservoir to develop the linear regression models. The TSS determined from Landsat images and the observed inflow volume to the Bokaa reservoir were used to quantify sediment yield from the Metsimotlhabe River catchment and the findings were correlated with the sediment yield obtained by the flow-calibrated ArcSWAT in Scenario 1 because it performed better than Scenario 2.

Table 11: Regression models used to retrieve TSS from Landsat images

No.	Regression Algorithm	Developed by:	R^2
1	$TSS = 368.7 \times \ln(R_{rs}\ (B3/B2)) + 31.52$	Nurandani et al. (2013)	0.956
2	$TSS = 698.6 \times R_{rs}\ (B4) – 0.83916$	Luan (2016)	0.920
3	$TSS = 602.63 \times (0.5157 \times R_{rs}\ (B4) – 0.0089) + 3.1481$	Rodríguez-guzmán & Gilbes-santaella (2009)	0.919
4	$TSS = 2.73 \times e^{3.11 \times R_{rs}\ (B4/B3)}$	Pham et al. (2018)	0.897

Note: B2 = band 2, 482nm; B3 = band 3, 562nm and B4 = band 4, 655nm

Four regression algorithms produced correlation factors higher than 0.8 (*Table 11*), with the lowest (0.897) being the fourth regression model used and the highest being the model developed by Nurandani et al. (2013) with an R^2 of 0.95. This algorithm adopted the ratio of B3/B2 as the regression parameter. It was utilized by Hariyanto et al. (2017) in a study in East Java, Indonesia, where an R^2 of 0.684 was obtained.

With all four algorithms, a very good relationship was achieved between the sediment yield simulated by the flow-calibrated ArcSWAT model and sediment yield derived from satellite images. The high R^2 correlations confirm the high potential of the Landsat band reflectance in estimating sediment yield (Pham et al., 2018) from the Metsimotlhabe River catchment and its accuracy may be improved by a correlation with the measured sediment yield in the future.

A comparison of sediment yield simulated by the flow-calibrated ArcSWAT and the best-performing regression algorithm (from Nurandani et al., 2013) is shown in *Figure 17*, together with R^2 (0.9557) and the linear regression equation that was produced.

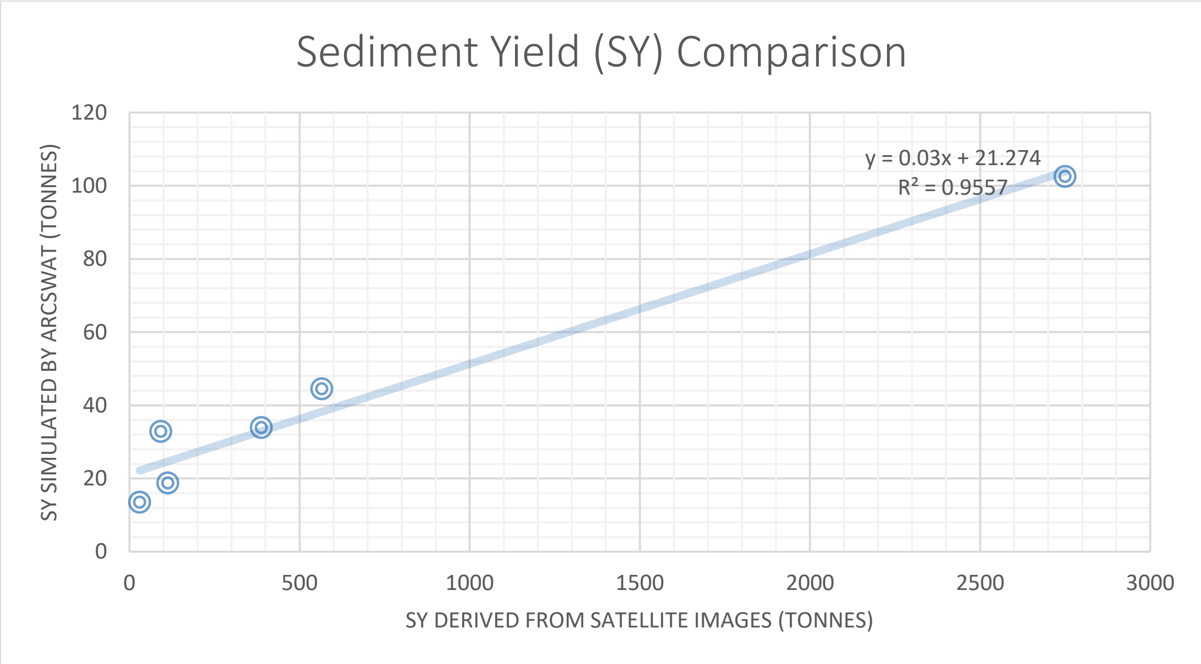

Figure 17: Correlation between simulated sediment yields (SY) from ArcSWAT and Landsat

A comparison of sediment yield simulated by the flow-calibrated ArcSWAT and the best-performed regression algorithm (No.1) is shown in *Figure 17* along with squared residual and the linear regression equation that was produced. A very good relationship was achieved between the sediment yield simulated by the flow-calibrated ArcSWAT and sediment yield derived from satellite images. The high correlations confirm the high potential of the Landsat band reflectance in estimating sediment yield (Pham et al., 2018) from the Metsimotlhabe River catchment and its accuracy may be improved by a correlation with the measured sediment yield in the future.

5. CONCLUSIONS AND RECOMMENDATIONS

5.1 CONCLUSIONS

The LULC of the Metsimotlhabe River catchment was successfully generated from Landsat images using PCI Geomatica and ArcGIS because the images had a satisfactory match with the ground truth data with a Kappa coefficient of 0.87 and 0.89. The ArcSWAT model was well-calibrated against the flow as indicated by the statistical analysis, this produced reasonable hydrologic simulation results concerning LULC, which could be used by water and environmental resources managers and policy and decision-makers.

The statistical analysis showed that the ArcSWAT model was well-calibrated against the flow. The R^2 for the calibration, validation and overall periods in Scenario 1 was 0.72, 0.89, and 0.82, respectively, whereas the R^2 for the calibration, validation, and overall periods in Scenario 2 were 0.69, 0.86, and 0.78, respectively. Scenario 1 and Scenario 2 produced peak simulated flows of 2.295 and 3.372 m^3/s, respectively.

The LULC change that occurred in the Metsimotlhabe River catchment between 2006 and 2018 was more significant because it produced larger peaks of flow and total sediment yield. These changes could be attributed to a 2.27% increase in built-up areas and an 8.0% and 7.89% decrease in forest and shrubland areas respectively due to the 2% increase in the annual population of people living around the watershed.

Positive relation with R^2 of 0.965 was achieved between the sediment yield simulated from the flow-calibrated ArcSWAT and sediment yield derived by applying RS spectral analysis. This study highlights the importance and practical applications of RS to overcome data scarcity in poorly monitored catchments by employing data acquired directly or indirectly from RS as inputs into SWAT. As a result, hydrologists and water resource managers can use RS approaches to conduct qualitative and quantitative studies of hydrological processes when data is insufficient.

5.2 RECOMMENDATIONS

The problem of missing weather data especially rainfall should be addressed by the upgrade of the hydrometric measuring stations to automation and by ensuring good maintenance. The departments of Meteorological Services and Sanitation & Water Affairs are trying but they are constrained by limited budgets and vandalism. Therefore, the government should provide the departments with more funding so that they can invest in upgrading, maintenance and security at the gauging stations since they provide important information for the nation.

More research should be conducted on the effects of different land-use and land cover classifications on sediment yield. This would allow the effects of changes in forest cover, barren land area, and built-up area on water flow and sediment yield to be quantified on an individual basis.

An *in-situ* assessment of water quality is required in the field of study to provide the real results that will support calibration and validation of ArcSWAT on the sediment amounts generated from the watershed. This is critical because without observed data, the simulation is of limited use.

6. REFERENCES

A Landsat Timeline « Landsat Science. (n.d.). Retrieved October 28, 2020, from https://landsat.gsfc.nasa.gov/a-landsat-timeline/

Abari, M. E., Majnounian, B., Malekian, A., & Jourgholami, M. (2017). Effects of forest harvesting on runoff and sediment characteristics in the Hyrcanian forests, northern Iran. *European Journal of Forest Research*, *136*, 375–386.

Abbaspour, K. C. (2015). *SWAT-CUP: SWAT Calibration and Uncertainty Programs - A User Manual.*

Abbaspour, K. C., Vaghefi, S. A., & Srinivasan, R. (2017). A guideline for successful calibration and uncertainty analysis for soil and water assessment: A review of papers from the 2016 international SWAT conference. *Water (Switzerland)*, *10*(6).

Abbaspour, K. C., Yang, J., Maximov, I., Siber, R., Bogner, K., Mieleitner, J., & Zobrist, J. (2007). Modelling hydrology and water quality in the pre-alpine / alpine Thur watershed using SWAT. *Journal of Hydrology, 333*, 413–430.

Abe, C. A. (2017). *SWAT Modelling of Streamflow and Sediment Concentration in an Amazonian Basin Impacted by Artisanal Mininggold*.

Abebe, T., & Gebremariam, B. (2019). Modeling runoff and sediment yield of Kesem dam watershed, Awash basin, Ethiopia. *SN Applied Sciences*, *1*(446).

Abusanina, O. E. L. (2018). *Hydrology and Phosphorus Model for Agricultural Watershed : SWAT simulation of Discharge and Nutrient Flux in the Medway Creek Watershed*. The University of Western Ontario.

Adeogun, A. G., Sule, B. F., & Salami, A. W. (2015). *Simulation of Sediment Yield At the Upstream Watershed of Jebba Lake in Nigeria Using Swat Model*. *27*(1), 25–40.

Aduna, T. (2009). *The Impact of Land-use/ Land Cover Change on Catchment Hydrology and Water Quality of Legedad-Dire Catchments, Ethiopia.*

Al-doski, J., Mansor, S., & Shafri, H. (2013). Change Detection Process and Techniques. *Civil and Environmental Research*, *3*(10), 37–46.

Alemaw, B. F., Majauale, M., & Simalenga, T. (2013). Assessment of Sedimentation Impacts on Small Dams—A Case of Small Reservoirs in the Lotsane Catchment. *Journal of Water*

Resource and Protection, *5*, 1127–1131.

Alemu, M. M. (2016). Integrated Watershed Management and Sedimentation. *Journal of Environmental Protection*, *7*, 490–494.

Anaba, L. A., Banadda, N., Kiggundu, N., Wanyama, J., Engel, B., & Moriasi, D. (2017). Application of SWAT to Assess the Effects of Land-use Change in the Murchison Bay Catchment in Uganda. *Computational Water, Energy, and Environmental Engineering*, *6*, 24–40.

Arnold, J. G., Moriasi, D. N., Gassman, P. W., Abbaspour, K. C., White, M. J., Srinivasan, R., Santhi, C., Harmel, R. D., Van Griensven, A., Van Liew, M. W., Kannan, N., & Jha, M. K. (2012). SWAT: Model use, calibration, and validation. *Transactions of the ASABE*, *55*(4), 1491–1508.

Arnold, J.G., Kiniry, J. R., Srinivasan, R., Williams, J. R., Haney, E. B., & Neitsch, S. L. (2007). *Soil Water Assessment Tool (SWAT)* (VERSION 20). Texas Water Resources Institute.

Arnold, Jeffrey G., Allen, P. M., & Bernhardt, G. (1993). A comprehensive surface-groundwater flow model. *Journal of Hydrology*, *142*, 47–69.

Asres, M. T., & Awulachew, S. B. (2010). SWAT based runoff and sediment yield modeling: A case study of the Gumera watershed in the Blue Nile basin. *Ecohydrology and Hydrobiology*, *10*(2–4), 191–199.

Babar, S., & Ramesh, H. (2015). Streamflow response to land-use-land cover change over the Nethravathi River Basin, India. *Journal of Hydrologic Engineering*, *20*(10).

Bakker, W. H., Feringa, W., Gieske, A. S. M., Gorte, B. G. H., Grabmaier, K. A., Hecker, C. A., Horn, J. A., Huurneman, G. C., Janssen, L. L. F., Kerle, N., Meer, F. D. van der, Parodi, G. N., Pohl, C., Reeves, C. V., Ruitenbeek, F. J. van, Schetselaar, E. M., Tempfl, K., Weir, M. J. C., Westinga, E., & Woldai, T. (2001). *Principles of Remote Remote Sensing* (K. Tempfli, N. Kerle, G. C. Huurneman, & L. L. F. Janssen (Eds.); Fourth edi). The International Institute for Geo-Information Science and Earth Observation (ITC).

Barnhart, B. L., Sawicz, K. A., Ficklin, D. L., & Whittaker, G. W. (2018). MOESHA: A Genetic Algorithm for Automatic Calibration and Estimation of Parameter Uncertainty and Sensitivity of Hydrologic Models. *Trans ASABE*, *60*(4), 1259–1269.

Beasley, D. B., Huggins, L. F., & Monke, E. J. (1980). ANSWERS : A Model for Watershed Planning. *Transactions of the ASAE*.

Bessah, E., Bala, A., Agodzo, S. K., Okhimamhe, A. A., Boakye, E. A., & Ibrahim, S. U. (2019). The impact of crop farmers' decisions on future land-use, land cover changes in Kintampo North Municipality of Ghana. *International Journal of Climate Change Strategies and Management*, *11*(1), 72–87.

Bieger, K., Hörmann, G., & Fohrer, N. (2013). The impact of land-use change in the Xiangxi Catchment (China) on water balance and sediment transport. *Regional Environmental Change*.

Bokaa Travel Information. (n.d.). Retrieved October 29, 2020, from https://www.botswana-info.com/country/town/951/bokaa

Bokan, L. T. (2015). *Simulation of Sediment Yield Using SWAT Model : A case of Kulekhani Watershed Lemma Tufa Bokan*.

Bonumá, N. B., Reichert, J. M., Rodrigues, M. F., Alberto, J., Monteiro, F., Arnold, J. G., & Srinivasan, R. (2015). Modeling Surface Hydrology, Soil Erosion, Nutrient Transport, and Future Scenarios with the Ecohydrological SWAT Model in Brazilian Watersheds and River Basins. *Tópicos Ci. Solo*, *9*, 241–290.

Boonkaewwan, S., & Chotpantarat, S. (2018). Impacts of land-use changes on watershed discharge and water quality in a large intensive agricultural area in Thailand. *Hydrological Sciences Journal*.

Botswana-Water-Sector-Policy-Brief. (2012). *Water Policy Brief Reflecting on the Challenges of Attaining a Green Economy for Botswana*.

Botswana Population (2020) - Worldometer. (n.d.). Retrieved October 23, 2020, from https://www.worldometers.info/world-population/botswana-population/

Botter, G., Porporato, A., Rodriguez-Iturbe, I., & Rinaldo, A. (2007). Basin-scale soil moisture dynamics and the probabilistic characterization of carrier hydrologic flows: Slow, leaching-prone components of the hydrologic response. *Water Resources Research*, *43*.

Bouraoui, F., Benabdallah, S., Jrad, A., & Bidoglio, G. (2005). Application of the SWAT model on the Medjerda river basin (Tunisia). *Physics and Chemistry of the Earth*, *30*, 497–507.

Boyle, D. P., Gupta, H. V., & Sorooshian, S. (2000). Toward improved calibration of hydrologic models: Combining the strengths of manual and automatic methods. *Water Resources Research*, *36*(12), 3663–3674.

Bresciani, M., Giardino, C., Stroppiana, D., Dessena, M. A., Buscarinu, P., Cabras, L., Schenk, K., Heege, T., Bernet, H., Bazdanis, G., & Tzimas, A. (2019). Monitoring water quality in two dammed reservoirs from multispectral satellite data. *European Journal of Remote Sensing*, *52*(sup4), 113–122.

Brezonik, P., Menken, K. D., Bauer, M., Brezonik, P., Menken, K. D., & Bauer, M. (2009). Landsat-based Remote Sensing of Lake Water Quality Characteristics, Including Chlorophyll and Colored Dissolved Organic Matter (CDOM). *Lake and Reservoir Management*, *21*(4), 373–382.

Central Statistical Office (CSO). (2012). *2011 Population & Housing Census*, *Preliminary Results Brief*. http://cso.gov.tt/publicationcontainer/2011-population-and-housing-census-preliminary-count/

Chandra, P., Patel, P. L., Porey, P. D., & Gupta, I. D. (2014). Estimation of sediment yield using SWAT model for Upper Tapi basin. *ISH Journal of Hydraulic Engineering*, *20*(3), 291–300.

Chaubey, I., Cotter, A. S., Costello, T. A., & Soerens, T. S. (2005). Effect of DEM data resolution on SWAT output. *Hydrological Processes*, *19*, 621–628.

Chiwera, B. (2015). *Effects of Land-use and Land Cover Change on Sediment Yield for Upper Sebakwe and Upper Nyazvidzi Sub- Catchments in Chikomba District*. MIDLANDS STATE UNIVERSITY.

Coffey, M. E., Workman, S. R., Taraba, J. L., & Fogle, A. W. (2004). Statistical procedures for evaluating daily and monthly hydrologic model predictions. *Biosystems and Agricultural Engineering Faculty Publications*, *157*.

Croke, B. F. W., Merritt, W. S., & Jakeman, A. J. (2004). A dynamic model for predicting hydrologic response to land cover changes in gauged and ungauged catchments. *Journal of Hydrology*, *291*, 115–131.

Dahlberg, A. C. (2000). Landscape(s) in transition: An environmental history of a village in North-east Botswana. *Journal of Southern African Studies*, *26*(4), 759–782.

Dang, A. T. N., & Kumar, L. (2017). Application of remote sensing and GIS-based hydrological modelling for flood risk analysis : a case study of District 8, Ho Chi Minh City, Vietnam. *Geomatics, Natural Hazards and Risk*, *5705*(November).

Daofeng, L., Ying, T., Changming, L., & Fanghua, H. (2004). Impact of land-cover and climate changes on runoff of the source regions of the Yellow River. *Journal of Geographical Sciences*, *14*(3), 330–338.

Dastrup, R. A., MA, & GISP. (2018). *Introduction to Physical Geography*.

de Andrade, M. P., & Ribeiro, C. B. de M. (2020). Impacts of land-use and cover change on paraíba do sul watershed streamflow using the swat model. *Revista Brasileira de Recursos Hidricos*, *25*(12).

Department of Water Affairs - Ministry of Minerals, E. & W., & Resources. (2013). *Botswana Integrated Water Resources Management & Water Efficiency Plan* (Vol. 1).

Devia, G. K., Ganasri, B. P., & Dwarakish, G. S. (2015). A Review on Hydrological Models. *Aquatic Procedia*, *4*, 1001–1007. https://doi.org/10.1016/j.aqpro.2015.02.126

Đorđević, B., & Dašić, T. (2011). Water Storage Reservoirs and their Role in the Development, Utilization and Protection of Catchment. *SPATIUM International Review*, *24*, 9–15.

dos Santos, F. M., de Oliveira, R. P., & Di Lollo, J. A. (2020). Effects of land-use changes on streamflow and sediment yield in Atibaia River Basin-SP, Brazil. *Water (Switzerland)*, *12*.

Duru, U. (2015). *Modeling Sediment Yield and Deposition Using the Swat Model: A Case Study of Cubuk I and Cubuk Ii Reservoirs, Turkey*. Colorado State University.

Dwarakish, G. S., & Ganasri, B. P. (2015). Impact of land-use change on hydrological systems: A review of current modeling approaches. *Cogent Geoscience*, *1*.

El-Sadek, A., & Irvem, A. (2014). Evaluating the impact of land-use uncertainty on the simulated streamflow and sediment yield of the Seyhan River basin using the SWAT model. *Turkish Journal of Agriculture and Forestry*.

El Ghonemy, M. R. (1998). Recent changes in agrarian reform and rural development strategies in the Near East. *FAO Paper Presented to the Rural Development International Workshop Held at in Godollo Hungary, 9 - 13 April 1996, p. 9.*, 179–191.

ERDAS IMAGINE: World-Class Remote Sensing Software | Hexagon Geospatial. (n.d.). Retrieved October 16, 2020, from https://www.hexagongeospatial.com/products/power-portfolio/erdas-imagine/erdas-imagine-remote-sensing-software-package

FAO. (2004). Drought impact mitigation and prevention in the Limpopo River Basin: A situation analysis. *Land and Water Discussion Paper 4*, *4*.

Ffolliott, P. F., Brooks, K. N., Pizarro, R., Pablo, T., Chevesich, G., & Neary, D. G. (n.d.). *Soil Erosion and Sediment Production on Watershed Landscapes: Processes, Prevention, and Control*.

Flanagan, D. C., Ii, J. C. A., Nicks, A. D., Nearing, M. A., & Laflen, J. M. (1995). *Chapter 1 . Overview of the WEPP Erosion Prediction Model*.

Flanagan, D. C., & Nearing, M. A. (1995). *USDA - Water Erosion Prediction Project Hillslope Profile and Watershed Model Documentation*.

Foley, J. A., DeFries, R., Asner, G. P., Barford, C., Bonan, G., Carpenter, S. R., Chapin, F. S., Coe, M. T., Daily, G. C., Gibbs, H. K., Helkowski, J. H., Holloway, T., Howard, E. A., Kucharik, C. J., Monfreda, C., Patz, J. A., Prentice, I. C., Ramankutty, N., & Snyder, P. K. (2005). Global consequences of land-use. *Science*, *309*, 570–574.

Foody, G. M. (2001). Monitoring the magnitude of land-cover change around the southern limits of the Sahara. *Photogrammetric Engineering and Remote Sensing*, *67*(7), 841–847.

Gao, F., Wang, Y., & Hu, X. (2018). Evaluation of the suitability of Landsat, MERIS, and MODIS for identifying spatial distribution patterns of total suspended matter from a self-organizing map (SOM) perspective. *Catena*, *172*, 699–710.

Gassman, P. W., Reyes, M. R., Green, C. H., & Arnold, J. G. (2007). The Soil and Water Assessment Tool: Historical Developments, Applications, and Future Research Directions. *Transactions of the ASABE*, *50*(4), 1211–1250.

Geomatica Training Guide. (2016). 136. http://www.pcigeomatics.com/pdf/training-guides/2016/Geomatica-1.pdf

Geremew, A. A. (2013). *Assessing the Impacts of Land-use and Land Cover Change on*

Hydrology of Watershed: A Case Study on Gilgel – Abbay Watershed, Lake Tana.

Getting Started With ENVI - [PDF Document]. (n.d.). Retrieved October 16, 2020, from https://vdocuments.site/documents/getting-started-with-envi.html

Goodarzi, E., Farhoudi, J., & Shokri, N. (2012). Flow Characteristics of Rectangular Broad-Crested Weirs with Sloped Upstream Face. *J. Hydrol. Hydromech.*, *60*(2), 87–100.

Govender, M., & Everson, C. S. (2005). Modelling streamflow from two small South African experimental catchments using the SWAT model. *Hydrological Processes*, *19*, 683–692.

Grath, B. (2016). *Simulation of Discharge and Nitrate-Nitrogen Loads in the Raab Catchment with the hydrological model SWAT* (Issue June). University of Natural Resources and Life Sciences, Vienna.

Guzha, A. C., Rufino, M. C., Okoth, S., Jacobs, S., & Nóbrega, R. L. B. (2018). Impacts of land-use and land cover change on surface runoff, discharge and low flows: Evidence from East Africa. *Journal of Hydrology: Regional Studies*, *15*, 49–67.

Hailu, C., Tamene, S., Demissie, A., & Gudu, F. (2020). Surface runoff modeling in Ketar watershed, Ethiopia. *Journal of Sedimentary Environments*.

Hansen, M. C., Egorov, A., Roy, D. P., Potapov, P., Ju, J., Turubanova, S., Kommareddy, I., & Loveland, T. R. (2011). Continuous fields of land cover for the conterminous United States using Landsat data: First results from the Web-Enabled Landsat Data (WELD) project. *Remote Sensing Letters*, *2*(4), 279–288.

Hariyanto, T., Krisna, T. C., Khomsin, Pribadi, C. B., & Anwar, N. (2017). Development of total suspended sediment model using landsat-8 OLI and In-situ data at the surabaya coast, East Java, Indonesia. *Indonesian Journal of Geography*, *49*, 73–79.

Huang, T., & Lo, K. (2015). Effects of Land-use Change on Sediment and Water Yields in Yang Ming Shan National Park, Taiwan. *Environments*, *2*, 32–42.

Im, S., Brannan, K. M., Mostaghimi, S., & Kim, S. M. (2007). Comparison of HSPF and SWAT models performance for runoff and sediment yield prediction. *Journal of Environmental Science and Health - Part A Toxic/Hazardous Substances and Environmental Engineering*, *42*(11), 1561–1570.

Imanparast, L., & Hassanpana, D. (2010). Soil Erodibility Effect on Sediment Producing in

Aras Sub Watershed. *Research Journal of Environmental Sciences*, *4*(2), 187–192.

Ismail, M. A., Muhamad Ludin, A. N., & Hosni, N. (2020). Comparative Assessment of the Unsupervised Land-use Classification by Using Proprietary GIS and Open Source Software. *IOP Conference Series: Earth and Environmental Science*, *540*.

Jaelani, L. M., Limehuwey, R., Kurniadin, N., Pamungkas, A., Koenhardono, E. S., & Sulisetyono, A. (2016). Estimation of Total Suspended Sediment and Chlorophyll-A Concentration from Landsat 8-Oli: The Effect of Atmosphere and Retrieval Algorithm. *IPTEK The Journal for Technology and Science*, *27*(1), 16–23.

Jain, M., & Tomar, P. S. (2013). Review of image classification methods and techniques. *International Journal Of Engineering Research and Technology*, *2*(8), 852–858. file:///C:/Users/SAV/Desktop/Thesis literature/image classification methods.pdf

Jones, M. O. (2006). *Application of MODIS for monitoring water quality of a large oligotrophic lake*. University of Montana.

Joshua, W. D. (1991). *Physical Properties of the Soils of Botswana*. http://www.fao.org/docrep/field/009/ar781e/ar781e.pdf

Kapalanga, T. S. (2015). *Assessment and Development of Remote Sensing Based Algorithms for Water Quality Monitoring in Olushandja Dam, North-Central Namibia Algorithms for Water Quality Monitoring in*. University of Zimbabwe.

Kebede, W. (2018). Effect of Soil and Water Conservation Measures and Challenges for its Adoption : Ethiopia in Focus. *Journal of Environmental Science and Technology*, *7*(4), 185–199. https://doi.org/10.3923/jest.2014.185.199

Keiner, M., & Cavric, B. I. (2004). *Managing the Development of a Fast Growing City: A case study of Gaborone, Botswana*.

Khan, T. H. (2014). *Water scarcity and its impact on agriculture*. Swedish University of Agricultural Sciences.

Khan, U., Kumar, N., & Sharma, A. (2013). Environmental Modelling & Software Delineating hydrologic response units in large upland catchments and its evaluation using soil moisture simulations. *Environmental Modelling and Software, 46*, 142–154.

Kimwaga, R. J., Bukirwa, F., Banadda, N., Wali, U. ., Nhapi, I., & Mashauri, D. A. (2012).

Modelling the Impact of Land-use Changes on Sediment Loading Into Lake Victoria Using SWAT Model: A Case of Simiyu Catchment Tanzania. *The Open Environmental Engineering Journal*, *5*(1), 66–76.

Kite, G. W., & Pietroniro, A. (1996). Remote sensing applications in hydrological modelling. *Hydrological Sciences Journal*, *41*(4), 563–591.

Knapp, H. V., Durgunoglu, A., & Ortel, T. W. (1991). A Review of Rainfall-Runoff Modeling for Stormwater Management. In *Illinois State Water Survey, Hydrology Division*.

Krause, P., Boyle, D. P., & Bäse, F. (2005). Comparison of different efficiency criteria for hydrological model assessment. *Advances in Geosciences*, *5*, 89–97.

Landsat Collection 2 Level-2 Science Products. (n.d.). Retrieved May 30, 2021, from https://www.usgs.gov/core-science-systems/nli/landsat/landsat-collection-2-level-2-science-products

Lenhart, T., Eckhardt, K., Fohrer, N., & Frede, H.-G. (2002). Comparison of two different approaches for making design sensitivity analysis an integrated part of finite element analysis. *Physics and Chemistry of the Earth*, *27*, 645–654.

Li, Y., Chang, J., Luo, L., Wang, Y., Guo, A., Ma, F., & Fan, J. (2018). Spatiotemporal impacts of land-use land cover changes on hydrology from the mechanism perspective using SWAT model with time-varying parameters. *Hydrology Research*.

Lin, B., Chen, X., Yao, H., Chen, Y., Liu, M., Gao, L., & James, A. (2015). Analyses of landuse change impacts on catchment runoff using different time indicators based on SWAT model. *Ecological Indicators*, *58*, 55–63.

Lin, Y. P., Hong, N. M., Wu, P. J., Wu, C. F., & Verburg, P. H. (2007). Impacts of land-use change scenarios on hydrology and land-use patterns in the Wu-Tu watershed in Northern Taiwan. *Landscape and Urban Planning*, *80*, 111–126.

Liu, J., Zhang, C., Kou, L., & Zhou, Q. (2017). Effects of Climate and Land-use Changes on Water Resources in the Taoer River. *Advances in Meteorology*.

Liu, Z., & Tong, S. T. Y. (2015). Using HSPF to Model the Hydrologic and Water Quality Impacts of Riparian Land-use Change in a Small Watershed. *Journal of Environmental Informatics*, *17*(1–14).

Loi, N. K. (2010). Assessing the Impacts of Land-use / Land cover Changes and Practices on Water Discharge and Sedimentation using SWAT : Case study in Dong Nai watershed – Vietnam. *International Symposium on Geoinformatics for Spatial Infrastructure Development in Earth and Allied Sciences 2010*.

Lu, D., & Weng, Q. (2007). A survey of image classification methods and techniques for improving classification performance. *International Journal of Remote Sensing*, *28*(5), 823–870.

Luan, X. B., Wu, P. Te, Sun, S. K., Li, X. L., Wang, Y. B., & Gao, X. R. (2018). Impact of Land-use Change on Hydrologic Processes in a Large Plain Irrigation District. *Water Resources Management*.

Ma, X., Xu, J., Luo, Y., Aggarwal, S. P., & Li, J. (2009). Response of hydrological processes to land-cover and climate changes in Kejie watershed, south-west China. *Hydrological Processes*, *23*, 1179–1191.

Madhav Narayan Shrestha. (2003). *Spatially Distributed Hydrological Modelling considering Land - use changes using Remote Sensing and GIS*.

Manandhar, R., Odehi, I. O. A., & Ancevt, T. (2009). Improving the Accuracy of Land-use and Land Cover Classification of Landsat Data Using Post-Classification Enhancement. *Remote Sensing*, *1*, 330–344.

Mango, L. M. (2010). *Modeling the Effect of Land-use and Climate Change Scenarios on the Water Flux of the Upper Mara River Flow, Kenya* [Florida International University].

Mao, Z., Chen, J., Pan, D., Tao, B., & Zhu, Q. (2012). Remote Sensing of Environment A regional remote sensing algorithm for total suspended matter in the East China Sea. *Remote Sensing of Environment*, *124*, 819–831.

Mas, J. F. (1998). *Monitoring land-cover changes: a comparison of change detection techniques*.

Matlhodi, B., Kenabatho, P. K., Parida, B. P., & Maphanyane, J. G. (2019). Evaluating land-use and land cover change in the Gaborone dam catchment, Botswana, from 1984-2015 using GIS and remote sensing. *Sustainability (Switzerland), 11*.

Mbajiorgu, C. C. (2018). Reservoir Sedimentation Modelling and Prediction of Project

Lifetime. *Journal of the Nigerian Academy of Engineering*, *1*(1), 28–41.

McGrane, S. J. (2016). Impacts of urbanisation on hydrological and water quality dynamics, and urban water management: a review. *Hydrological Sciences Journal*, *61*(13), 2295–2311.

Measuring instruments for sediment transport - Coastal Wiki. (n.d.). Retrieved August 5, 2020, from http://www.coastalwiki.org/wiki/Measuring_instruments_for_sediment_transport

Megnounif, A., Terfous, A., Ghenaim, A., & Poulet, B. (2007). Key processes influencing erosion and sediment transport in a semi-arid Mediterranean area : the Upper Tafna catchment , Algeria / Processus clefs bassin versant de la Haute Tafna , Algérie Key processes influencing erosion and sediment transport in a sem. *Hydrological Sciences*, *52*(6), 1271–1284.

Memarian, H., Balasundram, S. K., Abbaspour, K. C., Talib, J. B., Sung, C. T. B., & Sood, A. M. (2014). SWAT-based hydrological modelling of tropical land-use scenarios. *Hydrological Sciences*, *59*(10), 1808–1829.

Merritt, W. S., Letcher, R. A., & Jakeman, A. J. (2003). A review of erosion and sediment transport models. *Environmental Modelling and Software*, *18*, 761–799.

Miller, J. D., & Hess, T. (2017). Urbanisation impacts on storm runoff along a rural-urban gradient. *Journal of Hydrology*, *552*, 474–489.

Moriasi, D. N., Arnold, J. G., Liew, M. W. Van, Bingner, R. L., Harmel, R. D., & Veith, T. L. (2007). Model Evaluation Guidelines for Systematic Quantification of Accuracy in Watershed Simulations. *Transactions of the ASABE*, *50*(3), 885–900.

Moriasi, D. N., Wilson, B. N., Arnold, J. G., & Gowda, P. H. (2012). Hydrologic and Water Quality Models: Use, Calibration, and Validation. *Transactions of the ASABE*, *55*(4), 1241–1247.

Munoth, P., & Goyal, R. (2020). Impacts of land-use land cover change on runoff and sediment yield of Upper Tapi River Sub-Basin, India. *International Journal of River Basin Management*, *18*(2), 177–189.

Muttitanon, W., & Tripathi, N. K. (2005). Land-use/land cover changes in the coastal zone of Ban Don Bay, Thailand using Landsat 5 TM data. *International Journal of Remote*

Sensing, *26*(11), 2311–2323.

Ndulue, E. L., Mbajiorgu, C. C., Ugwu, S. N., Ogwo, V., & Ogbu, K. N. (2015). Assessment of land-use/cover impacts on runoff and sediment yield using hydrologic models: A review. *Journal of Ecology and The Natural Environment*, *7*(2), 46–55. https://doi.org/10.5897/jene2014.0482

Negese, A. (2021). *Impacts of Land-use and Land Cover Change on Soil Erosion and Hydrological Responses in Ethiopia*. *2021*, 10.

Negrel, J., Kosuth, P., & Bercher, N. (2011). Estimating river discharge from earth Observation measurement of river surface hydraulic variables. *Hydrology and Earth System Sciences*, *15*(6), 2049–2058.

Neitsch, S. ., Arnold, J. ., Kiniry, J. ., & Williams, J. . (2011). Soil & Water Assessment Tool Theoretical Documentation Version 2009. *Texas Water Resources Institute*, 1–647.

Niel, H., Paturel, J. E., & Servat, E. (2003). Study of parameter stability of a lumped hydrologic model in a context of climatic variability. *Journal of Hydrology*, *278*, 213–230.

Nilawar, A. P., & Waikar, M. L. (2018). Use of SWAT to determine the effects of climate and land-use changes on streamflow and sediment concentration in the Purna River basin, India. *Environmental Earth Sciences*, *77*(783).

Nkonge, L. K. (2017). *Assessment of the Transferability of Swat Model Parameters from Gauged to Ungauged Sub-Watersheds for Streamflow Simulation in the Upper Tana Watershed, Kenya*. Jomo Kenyatta University of Agriculture and Technology.

Nurandani, P., Subiyanto, I. S., & Sasmito, B. (2013). Mapping of Total Suspended Solid (TSS) Using Multi Temporal Satellite Imagery in Rawa Pening Lake, Central Java Province. *Geodesi Undip*.

Ongley, E. (1996). Chapter 13 - Sediment Measurements. In *Water Quality Monitoring - A Practical Guide to the Design and Implementation of Freshwater Quality Studies and Monitoring Programmes*.

Ouillon, S., Douillet, P., Petrenko, A., Neveux, J., Froidefond, J., Andréfouët, S., & Muñoz-Caravaca, A. (2008). Optical Algorithms at Satellite Wavelengths for Total Suspended Matter in Tropical Coastal Waters. *Sensors*, *8*, 4165–4185.

Palamuleni, L. G., Ndomba, P. M., & Annegarn, H. J. (2011). Evaluating land cover change and its impact on hydrological regime in Upper Shire river catchment, Malawi. *Regional Environmental Change*, *11*, 845–855.

Paul, S. (2015). *Assessment of change in future flow of Brahmaputra Basin applying SWAT model using multi-member ensemble climate data*. Bangladesh University of Engineering and Technology.

Pazúr, R., & Bolliger, J. (2017). Land changes in Slovakia : Past processes and future directions. *Applied Geography*, *85*, 163–175.

Pham, Q. V., Ha, N. T. T., Pahlevan, N., Oanh, L. T., Nguyen, T. B., & Nguyen, N. T. (2018). Using landsat-8 images for quantifying suspended sediment concentration in red river (Northern Vietnam). *Remote Sensing*, *10*.

Phetolo. (2009). *The Impact of Sand Extraction on River Flow*. University of Botswana.

Phinzi, K. (2018). *Spatio-Temporal Appraisal of Water-Borne Erosion Using Optical Remote Sensing and GIS in the Umzintlava Catchment (T32e), Eastern Cape, South Africa* [University of KwaZulu-Natal, South Africa].

Photogrammetry & Remote Sensing Software - PCI Geomatics. (n.d.). Retrieved October 16, 2020, from https://www.pcigeomatics.com/#

Pokhrel, B. K. (2018). Impact of land-use change on flow and sediment yields in the Khokana outlet of the Bagmati River, Kathmandu, Nepal. *Hydrology*, *5*(22).

Population & Housing Census 2011 Analytical Report. (2014).

Prabhanjan, A., Rao, E. P., & Eldho, T. I. (2015). Application of SWAT model and geospatial techniques for sediment-yield modeling in ungauged watersheds. *Journal of Hydrologic Engineering*.

Priyanka, & Patil, N. S. (2016). Runoff Modeling for Malaprabha Sub-Basin Using Swat Hydrological Model. *International Journal of Research in Engineering and Technology*, *5*(7), 35–38.

Quang, N. H., Sasaki, J., Higa, H., & Huan, N. H. (2017). Spatiotemporal variation of turbidity based on landsat 8 OLI in Cam Ranh Bay and Thuy Trieu Lagoon, Vietnam. *Water (Switzerland)*, *9*, 570.

Quyen, N. T. N., Liem, N. D., & Loi, N. K. (2014). Effect of land-use change on water discharge in Srepok watershed, Central Highland, Viet Nam. *International Soil and Water Conservation Research*, *2*(3), 74–86.

Raletshegwana. (2014). *The Effects of LULC Changes on Streamflow and Catchment Morphology in the Metsimotlhabe Catchment* [University of Botswana].

Reddy, A. S., & Reddy, M. J. (2015). *Evaluating the influence of spatial resolutions of DEM on watershed runoff and sediment yield using SWAT*. *124*(7), 1517–1529.

Reddy, M. A. (1996). Remote Sensing and Geographical Information Systems. In *Environmental Conservation* (Third eddi).

Refsgaard, J. C., Storm, B., & Clausen, T. (2010). Système Hydrologique Européen (SHE): Review and perspectives after 30 years development in distributed physically-based hydrological modelling. *Hydrology Research*, *41*(5), 355–377.

Rinsema, J. G. (2014). *Comparison of Rainfall- Runoff Models for Floods Forecastings*. University of the Tasmania.

Robert, E., Grippa, M., Kergoat, L., Pinet, S., Gal, L., Cochonneau, G., & Martinez, J. (2018). Monitoring water turbidity and surface suspended sediment concentration of the Bagre Reservoir (Burkina Faso) using MODIS and field reflectance data International Journal of Applied Earth Observation and Geoinformation Monitoring water turbidity and sur. *International Journal of Applied Earth Observations and Geoinformation*, *52*, 243–251.

Rodríguez-guzmán, V., & Gilbes-santaella, F. (2009). Using MODIS 250 m Imagery to Estimate Total Suspended Sediment in a Tropical Open Bay. *International Journal of Systems Applications, Engineering & Development*, *3*(1).

Samanta, S., & Pal, D. K. (2016). Change Detection of Land-use and Land Cover over a Period of 20 Years in Papua New Guinea. *Natural Science*, *8*, 138–151.

Schleiss, A. J., Franca, M. J., Juez, C., & De Cesare, G. (2016). Reservoir sedimentation. *Journal of Hydraulic Research*, *54*(6), 595–614.

Serra, P., Pons, X., & Saurí, D. (2003). Post-classification change detection with data from different sensors: Some accuracy considerations. *International Journal of Remote Sensing*, *24*(16), 3311–3340.

Setegn, S. G.; Dargahi, Srinivasan, R; and Melesse, A. M. . (2010). Modelling of Sediment Yield from Anjeni-gauged Watershed, Ethiopia using SWAT Model. *Journal of the American Water Resources Management*, *46*(3), 514–526.

Setegn, S. G., Srinivasan, R., & Dargahi, B. (2008). Hydrological Modelling in the Lake Tana Basin, Ethiopia Using SWAT Model. *The Open Hydrology Journal*, *2*, 49–62.

Singh, V. P. (2018). Hydrologic modeling: progress and future directions. *Geoscience Letters*, *5*(15).

Singh, V. P., & Frevert, D. K. (2003). Watershed Modeling. *World Water and Environmental Resources Congress*.

Sinha, R. K., & Eldho, T. I. (2018). Effects of historical and projected land-use/cover change on runoff and sediment yield in the Netravati river basin, Western Ghats, India. *Environmental Earth Sciences*, *77*(111).

Siregar, E. S. Y., Rahimah, I., Siregar, V. P., & Agus, S. B. (2019). Accuracy test of total suspended solid concentration by Landsat 8 on in-situ data in Lancang Island waters, Kepulauan Seribu. *Sixth International Symposium on LAPAN-IPB Satellite, 2019, Bogor, Indonesia*.

Sitterson, J., Knightes, C., Parmar, R., Wolfe, K., Muche, M., & Avant, B. (2017). An Overview of Rainfall-Runoff Model Types. In *United States Environmental Protection Agency*.

Son, N. T., Binh, Nguyen D., & Shrestha, R. P. (2015). Effects of Land-use Change on Runoff and Sediment Yield in Da River Basin of Hoa Binh province, Nonorthwest Vietnam. *J. Mt. Sci.*, *12*(4), 1051–1064.

Statistics-Botswana. (2016). *Botswana Environment Statistics*.

Story, M., & Congalton, R. G. (1986). Accuracy Assessment: A User's Perspective. *Photogrammetric Engineering and Remote Sensing*, *52*(3), 397–399.

Sui, D. Z., & Maggio, R. C. (1999). Integrating GIS with hydrological modeling : practices, problems, and prospects. *Computers, Environment and Urban Systems*, *23*, 33–51.

Supervised and Unsupervised Classification in Remote Sensing - GIS Geography. (n.d.). Retrieved October 20, 2020, from https://gisgeography.com/supervised-unsupervised-classification-arcgis/

Tang, L., Yang, D., Hu, H., & Gao, B. (2011). Detecting the effect of land-use change on streamflow, sediment and nutrient losses by distributed hydrological simulation. *Journal of Hydrology*, *409*, 172–182.

Teodoro, A. C., Ferreira, D., & Sillero, N. (2012). Performance of commercial and open source remote sensing/image processing software for land cover/use purposes. *Earth Resources and Environmental Remote Sensing/GIS Applications III*, *8538*.

Tolosa, D. (2015). *Modelling Sediment Yield using ArcSWAT and Analyzing the most Prominent Remedial Measures: Cases of Melka Wakena Reservoir, Ethiopia*. Addis Ababa University.

Tsheko, R. (2006). Comparison between the United States Soil Conservation Service (SCS) and the two models commonly used for estimating rainfall-runoff in south-eastern Botswana. *Water SA*, *32*(1), 29–36.

Unsupervised classification. (n.d.). Retrieved October 20, 2020, from https://www.pcigeomatics.com/geomatica-help/concepts/focus_c/oa_classif_intro_unsuperClass.html

Unsupervised Classification []. (n.d.). Retrieved October 20, 2020, from https://wiki.landscapetoolbox.org/doku.php/remote_sensing_methods:unsupervised_classification

Van Rompaey, A. J. J., Govers, G., & Puttemans, C. (2002). Modelling land-use changes and their impacts on soil erosion and sediment supply to rivers. *Earth Surface Processes and Landforms*, *27*, 481–494.

Vaze, J., Jordan, P., Beecham, R., Frost, A., & Summerell, G. (2011). *Guidelines for Rainfall-Runoff Modelling: Towards Best Practice Model Application*. eWater Cooperative Research Centre.

Wagener, T., & Wheater, H. S. (2006). Parameter estimation and regionalization for continuous rainfall-runoff models including uncertainty. *Journal of Hydrology, 320*, 132–154.

Wang, G., Liu, J., Kubota, J., & Chen, L. (2007). Effects of land-use changes on hydrological processes in the middle basin of the Heihe River, northwest China. *Hydrological Processes*, *21*, 1370–1382.

Wang, X., & Yang, W. (2019). Water quality monitoring and evaluation using remote-sensing techniques in China: A systematic review. *Ecosystem Health and Sustainability*, *5*(1), 47–56.

What is Data Validation? How It Works and Why It's Important. (n.d.). Retrieved October 21, 2020, from https://www.safe.com/what-is/data-validation/

Wijesekera, N. T. S., & Perera, L. R. H. (2012). Key Issues of Data and Data Checking for Hydrological Analyses - Case Study of Rainfall Data in the Attanagalu Oya Basin of Sri Lanka. *Engineer: Journal of the Institution of Engineers, Sri Lanka*, *45*(2), 1–12.

Winchell, M., Srinivasan, R., Di Luzio, M., & Arnold, J. (2010). *ArcSWAT interface for SWAT2009 User's Guide*.

Wolancho, K. W. (2012). Watershed management: An option to sustain dam and reservoir function in Ethiopia. *Journal of Environmental Science and Technology*.

Woldesenbet, T. A., Elagib, N. A., Ribbe, L., & Heinrich, J. (2016). Hydrological responses to land-use / cover changes in the source region of the Upper Blue Nile Basin, Ethiopia. *Science of the Total Environment*.

Wong, M. S., Nichol, J. E., Lee, K. H., & Emerson, N. (2005). Modeling Water Quality Using Terra / MODIS 500m Satellite Images. *The International Archives of the Photogrammetry, Remote Sensing and Spatial Information Sciences*, *37*, 679–684.

Worku, T., Khare, D., & Tripathi, S. K. (2017). Modeling runoff–sediment response to land-use/land cover changes using integrated GIS and SWAT model in the Beressa watershed. *Environmental Earth Sciences*, *76*.

Xiaoming, Z., Xinxiao, Y., Sihong, W., & Huifang, L. (2007). *Effects of forest vegetation on runoff and sediment transport of watershed in Loess area, west China*. *2*(2), 163–168.

Xu, Z. X., Pang, J. P., Liu, C. M., & Li J.Y. (2009). Assessment of runoff and sediment yield in the Miyun Reservoir catchment by using SWAT model. *Hydrologycal Processes*, *23*, 3619–3630.

Yalew, S., Teferi, E., Griensven, A. Van, Uhlenbrook, S., & Mul, M. (2012). Land-use Change and Suitability Assessment in the Upper Blue Nile Basin Under Water Resources and Socio-economic Constraints : A Drive Towards a Decision Support System. *International*

Environmental Modelling and Software Society (IEMSs).

Yan, B., Fang, N. F., Zhang, P. C., & Shi, Z. H. (2013). Impacts of land-use change on watershed streamflow and sediment yield: An assessment using hydrologic modelling and partial least squares regression. *Journal of Hydrology*, *484*, 26–37.

Yang, X., Liu, Q., He, Y., Luo, X., & Zhang, X. (2015). Comparison of daily and sub-daily SWAT models for daily streamflow simulation in the Upper Huai River Basin of China. *Stochastic Environmental Research and Risk Assessment*.

Yesuf, H. M., Assen, M., Alamirew, T., & Melesse, A. M. (2015). Modeling of sediment yield in Maybar gauged watershed using SWAT, northeast Ethiopia. *Catena*, *127*, 191–205.

Ying, Q., Hansen, M. C., Potapov, P. V., Tyukavina, A., Wang, L., Stehman, S. V., Moore, R., & Hancher, M. (2017). Global bare ground gain from 2000 to 2012 using Landsat imagery. *Remote Sensing of Environment*, *194*, 161–176.

Yousuf, A. and Singh, M. J. (2016). Runoff and soil loss estimation using hydrological models, remote sensing and GIS in Shivalik foothills : a review. *Journal of Soil and Water Conservation*, *15*(3), 205–210.

Yu, D., Shi, P., Liu, Y., & Xun, B. (2013). Detecting land-use-water quality relationships from the viewpoint of ecological restoration in an urban area. *Ecological Engineering*, *53*, 205–216.

Yu, M., Chen, X., Li, L., Bao, A., & de la Paix, M. J. (2011). Streamflow Simulation by SWAT Using Different Precipitation Sources in Large Arid Basins with Scarce Raingauges. *Water Resources Management*, *25*, 2669–2681.

Yuan, L., & Forshay, K. J. (2019). Using SWAT to evaluate streamflow and lake sediment loading in the xinjiang river basin with limited data. *Water (Switzerland)*, *12*(39).

Zhang, L., Meng, X., Wang, H., & Yang, M. (2019). Simulated runoff and sediment yield responses to land-use change using the SWAT model in Northeast China. *Water (Switzerland)*, *11*(915).

Zhang, Z., Wang, S., Sun, G., McNulty, S. G., Zhang, H., Li, J., Zhang, M., Klaghofer, E., & Strauss, P. (2008). Evaluation of the MIKE SHE model for application in the Loess Plateau, China. *Journal of the American Water Resources Association*, 1108–1120.